The potential effect of iontophoresis technology on the delivery of various melanoma vaccines into the skin

2023

Tokushima University

Graduate School of Pharmaceutical Sciences

Rabab Ahmed ZeinElAbdin Husseini

List of Contents

List of Tables…….. **I**

List of Figures……. **II**

List of abbreviations…….. **III**

Abstract……... **VI**

Chapter I: Introduction……. **1**

1.1. Cancer immunotherapy……. 1

1.2. Challenges for the transdermal delivery of biological macromolecules……..... 2

1.3. Trials toward overcoming the hurdles related to the transdermal delivery……... 4

1.4. Iontophoresis technology…….. 5

1.5. Application of iontophoresis……. 6

Chapter II: The Effect of Iontophoretic-Delivered Polyplex Vaccine on Melanoma Regression…… **9**

2.1. Introduction……... 9

2.2. Materials and Methods……... 13

2.2.1. Materials……. 13

2.2.2. Animal and tumor cells…….. 14

2.2.3. Preparation of polyplex nanoparticles……..... 14

2.2.4. Iontophoresis of fluorescent-labeled polyplex nanoparticles……. 15

2.2.5. Effect of iontophoresis on intradermal distribution of fluorescent-labeled polyplexes…… 16

2.2.6. *In vivo* vaccination for prophylactic studies…….. 16

2.2.7. RNA extraction…….. 17

2.2.8. Quantitative analysis of mRNA expression levels of inflammatory cytokines in different tissues using RT-PCR…… 17

2.2.9. Immunohistochemistry analysis of infiltrated $CD8^+$ and $CD4^+$ T cells in tumor tissue after pre-immunization with iontophoretic-administered polyplexes…… 18

2.2.10. *In vivo* vaccination for long-term prophylactic study ……. 18

2.2.11. *In vivo* vaccination by polyplexes for therapeutic studies …….. 19

2.2.12. ELISA…….. 19

2.2.13. Statistical analysis…… 19

2.3. Results…….. 20

2.3.1. Preparation of polyplex nanoparticles…….. 20

2.3.2. Iontophoresis of fluorescent-labeled polyplex nanoparticles……... 20

2.3.3. Effect of iontophoretic-administered prophylactic polyplex vaccine on melanoma inhibition…… 22

2.3.4. The role of cytokines production and infiltration of cytotoxic $CD8^+$ T cells in inhibiting melanoma growth after pre-immunization with iontophoretic-administered polyplex vaccine…….. 25

2.3.5. Effect of long-lasting immunity on melanoma regression after pre-immunization with iontophoretic-administered polyplex vaccine……... 27

2.3.6. Effect of iontophoretic-delivered therapeutic polyplex vaccine on cytokines production and melanoma inhibition……... 28

2.3.7. Iontophoretic delivery of therapeutic polyplex vaccine enhanced systemic immunity…….. 31

2.4. Discussion……... 33

2.5. Conclusion…….. 40

Chapter III: Use of Iontophoresis Technology for Transdermal Delivery of a Minimal mRNA Vaccine as a Potential Melanoma Therapeutic…….. 41

3.1. Introduction……... 41

3.2. Materials and Methods…….. 44

3.2.1. Materials…….. 44

3.2.2. Animal and tumor cells…… 45

3.2.3. Iontophoresis technology for delivery of FITC-labeled oligonucleotide……... 45

3.2.4. Intradermal distribution of FITC-labeled oligonucleotide after applying iontophoresis…… 46

3.2.5. Preparation of minimal naked mRNA vaccine as a potential melanoma therapeutic…… 46

3.2.6. Therapeutic effect of iontophoretic-delivered minimal mRNA vaccine on tumor regression……... 47
3.2.7. RNA extraction……..... 48
3.2.8. RT-PCR for quantitative analysis of various cytokines in different tissues…….. 48
3.2.9. Investigation of infiltrated cytotoxic $CD8^+$ and $CD4^+$ T cells in the tumor and spleen tissues by immunohistochemistry analysis……...…… 48
3.2.10. ELISA……..……..... 49
3.2.11. Statistical analysis…… 49
3.3. Results……... 50
3.3.1. Iontophoresis of fluorescent-labeled oligonucleotide…… 50
3.3.2. Effect of iontophoretic-administered therapeutic minimal mRNA vaccine on melanoma inhinbition…….…… 51
3.3.3. The role of cytokines production and infiltration of cytotoxic $CD8^+$ T cells in inhibiting melanoma growth after immunization with iontophoretic-administered minimal mRNA vaccine……... 53
3.3.4. Iontophoretic delivery of therapeutic minimal mRNA vaccine enhanced systemic immunity……... 57
3.4. Discussion …… 58
3.5. Conclusion…… 61
Chapter IV: Conclusion and Future Perspectives…….. 62
Acknowledgments & Dedication……. 63
References……... 64

List of Tables

Table 2.1. Primer sequences used for reverse transcription polymerase chain reaction (RT-PCR)……. 14

Table 2.2. Physicochemical properties of polyplex nanoparticles prepared at different N/P ratios……. 20

List of Figures

Fig 1.1. Schematic illustration of skin's layers…… 4

Fig 1.2. Iontophoresis technology…….... 5

Fig 2.3. Distribution of fluorescent-labeled polyplexes in skin tissue after IP application…… 21

Fig 2.4. Deep penetration of Cy3-labeled CpG-ODN in skin tissue after IP application…… 22

Fig 2.5. Effect of pre-immunization with prophylactic vaccines on tumor regression… 24

Fig 2.6. Quantitative analysis of mRNA expression levels of inflammatory cytokines in different tissues of prophylactic vaccinated mice…… 26

Fig 2.7. Immunohistochemical detection of infiltrated cytotoxic $CD8^+$ and $CD4^+$ T cells in tumor tissue…….. 27

Fig 2.8. Influence of the long-term prophylactic effect of polyplex vaccine on tumor regression …… 28

Fig 2.9. Anti-tumor effect of the therapeutic polyplex vaccine in mice bearing melanoma……. 29

Fig 2.10. Quantitative analysis of mRNA expression levels of inflammatory cytokines in different tissues of mice bearing melanoma treated with the polyplex vaccine…….. 30

Fig 2.11. Detection of IFN-γ levels at different time intervals in the serum of mice bearing melanoma treated with the polyplex vaccine…….. 32

Fig 3.12. Intradermal distribution of FITC-labeled oligonucleotide (green) after IP application…… 50

Fig 3.13. Therapeutic effect of minimal mRNA vaccine on tumor inhibition……. 52

Fig 3.14. Quantitative analysis of mRNA expression levels of inflammatory cytokines in different tissues of mRNA-vaccinated mice…… 54

Fig 3.15a. Immunohistochemical detection of infiltrated cytotoxic $CD8^+$ and $CD4^+$ T cells in tumor tissue…….. 55

Fig 3.15.b. Immunohistochemical detection of infiltrated cytotoxic $CD8^+$ and $CD4^+$ T cells in spleen tissue……. 56

Fig 3.16. Detection of serum IFN-γ levels at different time intervals in mice bearing melanoma treated with the minimal mRNA vaccine……... 57

List of abbreviations

Human gp100	Human glycoprotein 100
CpG-ODN	Cytosine-phosphate-guanosine oligodeoxynucleotide
siRNA	Small interfering RNA
IP	Iontophoresis
LCs	Langerhans cells
mRNA	Messenger RNA
IFN-γ	Interferon gamma
$CD8^+$ T cells	Cluster of differentiation 8 T cells
APCs	Antigen-presenting cells
FDA	Food and drug administration
s.c	Subcutaneous
IL	Interleukin
TNF-α	Tumor necrosis factor-alpha
HSP47	Heat shock protein 47
Pdx-1	Pancreatic and duodenal homeobox-1
Ccl4	Carbon tetra chloride
USA	United States of America
CTCA	Cancer treatment centers of America®
NCI	National cancer institute
DCs	Dendritic cells
HBV	Hepatitis B virus
HPV	Human papilloma virus
UK	United Kingdom
TSAs	Tumor specific antigens
TAAs	Tumor associated antigens
MHC	Major histocompatibility complex
TLR9	Toll like receptor 9
$CD4^+$ T cells	Cluster of differentiation 4 T cells
Cy3	Sulfo-Cyanine3
FITC	Fluorescein isothiocyanate

OCT	Optimal cutting temperature
DAPI	4',6-Diamidino-2-phenylindole, dihydrochloride
RT Master Mix	Real Time master mix
BSA	Bovine serum albumin
ELISA	Enzyme-linked immunosorbent assay
IgG	Immunoglobulin G
RT-PCR	Reverse transcription polymerase chain reaction
GAPDH	Glyceraldehyde-3-phosphate dehydrogenase
C57BL/6J	Common inbred strain of laboratory mouse
B16F1	Mouse melanoma cell line
DMEM	Dulbecco's modified Eagle's medium
FBS	Fetal bovine serum
CO2	Carbon dioxide
µl	Microliter
µg	Microgram
N/P ratio	Ratio of positively-chargeable polymer amine (N = nitrogen) groups to negatively-charged nucleic acid phosphate (P) groups
PDI	Polydispersity index
PBS	Phosphate buffer solution
Ag-AgCl	Silver-silver chloride
MAS	Matsunami
CLSM	Confocal laser scanning microscope
mA	Milliampere
T_{vol}	Tumor volume
cDNA	Complementary DNA
mV	Millivolt
M.W	Molecular weight
ANOVA	Analysis of variance
S.D	Standard deviation
DLNs	Draining lymph nodes

Th-1	T helper-1
CTLs	Cytotoxic T lymphocytes
Pg	Picogram
HIV	Human immunodeficiency virus
ORF	Open reading frame
CRISPR/Cas9	Clustered regularly interspaced short palindromic repeats/ CRISPR-associated protein 9
RP-HPLC	Reversed-phase HPLC
TBAF	Tetrabutylammonium fluoride
THF	Tetrahydrofuran
m^7GDP	7-methylguanosine diphosphate imidazolide
DMSO	Dimethyl sulfoxide

Abstract

Abstract

Recently, immunotherapy has attracted the attention toward enhancing cancer management strategies based on the unique features of the immune system. Although the fundamental strategy in cancer vaccination is to provide a therapeutic effect against an established tumor, there is an urgent need to develop prophylactic vaccines with a long-term memory for non-viral cancers. In this study, I prepared negatively charged polyplex nanoparticles through electrostatic interactions between a positively-charged modified tumor associated antigen, namely human derived melanoma $gp100_{25\text{-}33}$ peptide (KVPRNQDWL-RRRR), and a negatively charged cytosine-phosphate-guanosine oligodeoxynucleotide motif (CpG-ODN) adjuvant. My laboratory previously demonstrated successful transdermal delivery of various hydrophilic macromolecules, including small interfering RNA (siRNA), CpG-ODN and charged liposomes, by iontophoresis (IP) using weak electricity. Herein, I investigated the effectiveness of IP in the transdermal delivery of a prophylactic polyplex vaccine for activating skin-resident immune cells. Non-invasive IP was successful in establishing a homogenous distribution of the prophylactic cancer vaccine throughout the skin. Efficacy of the prophylactic vaccine delivered either by IP or subcutaneous (s.c) injection was demonstrated in pre-immunized mice by induction of immune cells against melanoma growth. A significant tumor regression effect was observed, which was confirmed by elevated messenger RNA (mRNA) expression levels of various cytokines in the tumor tissue, mainly interferon (IFN)-γ, as well as infiltration of cytotoxic $CD8^+$ and $CD4^+$ T cells. Additionally, I evaluated the therapeutic effect of the vaccine against mice bearing melanoma and I found a significant (80%) reduction in tumor burden. Stimulation of systemic immunity was also confirmed by upregulation of serum IFN-γ. Finally, results showed a non-significant difference between IP and s.c injection.

Unlike DNA vaccines, mRNA vaccines lack the possibility for genomic integration, resulting in minimal concerns for gene disruption, mutagenesis and tumorigenesis. Moreover, mRNA vaccines are distinguished by their short half-lives and well-tolerated safety profile, as well as their rapid, high-yield, safe, and cost-effective production. Additionally, mRNA vaccines have attracted considerable attention as a result of the 2019 coronavirus pandemic; however, challenges remain regarding use of mRNA vaccines, including insufficient delivery owing to the high molecular weights and high negative charges associated with mRNA. These characteristics of mRNA vaccines impair intracellular uptake and subsequent protein translation. Therefore, I examined the effect of IP technology on the delivery of mRNA vaccine into skin layers. In this study, a minimal mRNA vaccine encoding a tumor associated antigen human $gp100_{25\text{-}33}$ peptide (KVPRNQDWL), as a potential treatment for melanoma was chemically synthesized. Minimal mRNA vaccines have recently shown promise at improving the translational process, and can be prepared via a simple production method. Moreover, my laboratory previously reported the successful use of IP technology in the intracellular delivery of siRNA. I hypothesized that combining IP technology with a chemically synthesized minimal mRNA vaccine can improve both transdermal and intracellular delivery of mRNA vaccine. Therapeutic minimal mRNA vaccine was administered either by IP or s.c injection. Following IP-induced delivery of a minimal mRNA vaccine, an immune response is elicited resulting in activation of skin resident immune cells. As expected, combining both technologies led to potent stimulation of the immune system, which was observed via potent tumor inhibition in mice bearing melanoma. Additionally, there was an elevation in mRNA expression levels of various cytokines, mainly IFN-γ, as well as infiltration of cytotoxic $CD8^+$ and $CD4^+$T cells in the tumor tissue, which are responsible for tumor clearance. Also, stimulation of systemic immunity was confirmed by upregulation of serum IFN-γ level. Finally, minimal mRNA vaccine showed a Potent and

higher effect after using IP technology compared to the s.c injection. This is the first report which combines IP technology with a chemically synthesized minimal mRNA vaccine.

Overall, the obtained results indicate the effectiveness of the IP-administered prophylactic polyplex vaccine to act as a safe, immunogenic agent and stimulate immune cells to fight against melanoma growth. Moreover, IP technology improved the delivery of minimal mRNA vaccine into skin layers and the intracellular uptake by antigen presenting cells (APCs).

Chapter I

Introduction

Chapter I: Introduction

1.1. Cancer immunotherapy

Cancer is a complex disease characterized by the uncontrolled amplification of abnormal cells in the body [1]. The cancer-related mortality rate is expected to reach 22 million by 2030 [2]. According to the type and the stage of cancer, a convenient treatment strategy will be considered [2]. Generally, cancer treatment strategies include surgery, chemotherapy, radiotherapy, and a combination of these approaches. Chemotherapeutic agents can be used alone as the first line treatment for therapeutic purposes or in combination with surgery or radiotherapy to reduce the tumor volume before the surgery or inhibit cancer cell proliferation [2,3]. Nowadays, although it is possible to treat cancer with various treatment methods, the desired success rate in cancer treatment has not yet been achieved [2,3]. This is due to the undesirable side effects and systemic toxicity of cancer treatments, especially chemotherapy. Accordingly, various strategies have been developed to overcome these serious side effects and achieve a more effective therapy [3]. Recently, immunotherapy has attracted attention toward enhancing cancer management strategies based on the unique features of the immune system [2,4]. In a broader sense, the strategy of cancer immunotherapy is relying on the sensitization of the patient's immune system to cancer, which increases selectivity and reduces side effects [4]. Cancer immunotherapy's efficacy has been proven not only in *in vitro* and *in vivo* studies but also in the clinical trials which led to the selection of cancer immunotherapy as the "2013 Breakthrough of the Year" by Science [5]. Moreover, Food and Drug Administration (FDA) has approved various cancer immunotherapeutic drugs [2]. On the other hand, like other treatment methods, cancer immunotherapies have some restrictions, such as induction of immune reaction against normal tissues, the development of resistance, high treatment cost, the evaluation of treatment

efficacy, and the delivery system [6-8]. Herein, I will focus on the problem related to the delivery of cancer immunotherapies. The use of nanocarrier systems for the delivery of cancer immunotherapies showed an improvement in the stimulation of the immune system compared with conventional immunotherapy. This stimulation was through various mechanisms such as targeting specific immune cells, activating and enabling immune cells to recognize cancer cells, protecting the active molecule from biological factors, and effectively delivering to cancer tissues [2,9,10]. Although the delivery by nanoparticles holds promise for cancer immunotherapy, some limitations must be taken into consideration. The toxicity characteristics of nanoparticle-based immunotherapy require adequate attention [11]. It is ambiguous whether nanoparticles increase immune stimulation and autoimmune responses [11]. Moreover, nanotechnology can increase the complexity and cost of manufacture, and commercialization, which are detrimental to the clinical translation of nanoparticle-based immunotherapy [11]. Finally, invasive routes which used for the delivery of these nanosystems have undesirable characteristics.

1.2. Challenges for the transdermal delivery of biological macromolecules

In recent years, biological macromolecular therapeutics such as peptides, proteins, and nucleic acids have been considered significant therapeutic patterns for various diseases [12-14].These therapeutics are characterized by their specificity and convenient safety [15].On the other hand, such therapeutics have restrictions, including poor oral bioavailability and short half-lives [16]. Although invasive drug delivery routes, such as intradermal injection, subcutaneous (s.c) injection, and intravenous injection, have been recognized as efficient delivery routes, they are also associated with undesirable characteristics, such as invasiveness, pain, patient phobia, vagal reflex, risk of infection, and require special training [17-20]. Accordingly, alternative non-invasive transdermal routes have been utilized to deliver such drugs [15,21-23]. Despite the merits associated with non-invasive transdermal delivery, there

are hurdles that restrict the delivery of macromolecules into the skin. Especially the stratum corneum represents the outermost layer of the skin and hinders the permeation of hydrophilic macromolecules into the skin [24].

It is known that the skin is considered the largest organ in the body, and its surface area represents (1.7 m^2) which offers a vast surface area for drug administration [25]. In addition to the conveniences and accessibility of the transdermal route, this route bypasses the hepatic first-pass effect. It protects the drugs from degradation by gastric enzymes compared to the other routes [26,27]. Also, high concentrations of biological macromolecular drugs can be applied by this route, and various skin diseases can be managed [16].

The skin comprises two main layers: the epidermis and dermis (**Fig. 1.1**) [16]. The skin appendages include hair follicles, sweat glands, and sebaceous glands [28]. The outermost layer of the epidermis is known as the horny layer or the stratum corneum layer, which represents 10-15 μm thick and consists of corneocytes [24,29]. Corneocytes are non-living cells arranged by a network of proteins and enclosed by a lipid layer, and these make the stratum corneum provides a skin's natural protective barrier [29,30]. Additionally, corneocytes are known for the self-renewal process in which they subrogate persistently, aiming to keep the integrity of the stratum corneum [29]. The self-renewal process can negatively affect the absorbed drugs by pushing them outside the body [15]. Additionally, small hydrophobic drugs can permeate via the lipid layer of the stratum corneum, while hydrophilic macromolecules cannot diffuse [31]. Therefore, stratum corneum is a tough challenge for crossing biological macromolecules into the skin [32].

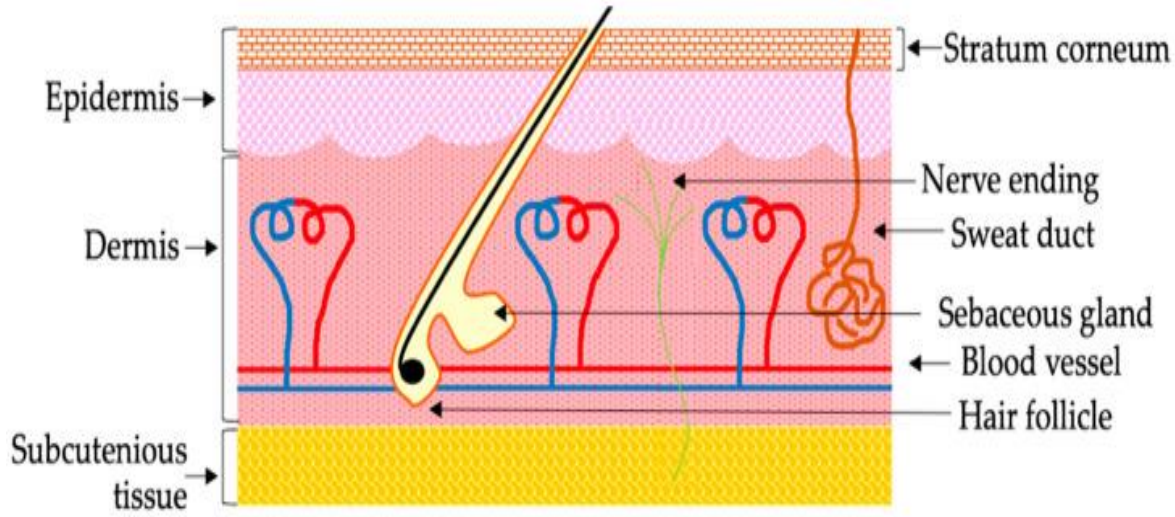

Fig 1.1. Schematic illustration of skin's layers.

Hasan M, Khatun A, Kogure K. Iontophoresis of Biological Macromolecular Drugs. Pharmaceutics., 14, 1-16 (2022).

1.3. Trials toward overcoming the hurdles related to the transdermal delivery

Several approaches have been examined in a trial toward overcoming the stratum corneum's difficulties in drug delivery, such as chemical and physical improvement methods [33]. First, chemical enhancer methods include using organic solvents, fatty acids glycol, and surfactants, which aim to induce a change in the lipid structure and enhance the stratum corneum's permeability [34]. Additionally, lipid- and polymeric-based nanoparticle formulations have been investigated broadly [35-37]. It has been demonstrated that these enhancing methods slightly improved the delivery of biological macromolecules into the skin. However, chemical enhancers have some hurdles, such as skin irritation, and negatively affect the release of the encapsulated drug and its activity [38,39]. Second, physical methods, which rely mainly on inducing disruption or bypassing the skin barriers, such as iontophoresis (IP), electroporation, ultrasound, and microneedles, showed great progress in the delivery of biological macromolecules into the skin [40-45].

Among these mentioned transdermal delivery methods, I will focus on IP technology owing to its unique features, such as simplicity, non-complicated application, and the lack of cytotoxicity.

1.4. Iontophoresis technology

The non-invasive technology of IP depends on applying an acceptable weak electric current, usually <0.5 mA/cm^2, for enhancing the transdermal delivery of hydrophilic and charged molecules of low molecular weights [46,47]. In general, the system of IP consists of negatively (cathode) and positively (anode) charged electrodes, a drug reservoir, an electronic controller, and a power source (**Fig. 1.2**) [16,48]. Usually, the electrode which contains the drug reservoir is known as the active electrode, and the second electrode is called the return electrode, which contains the counter ions [49]. Both electrodes are attached to the skin surface with a 1 cm distance in between to complete the electric circuit [49].

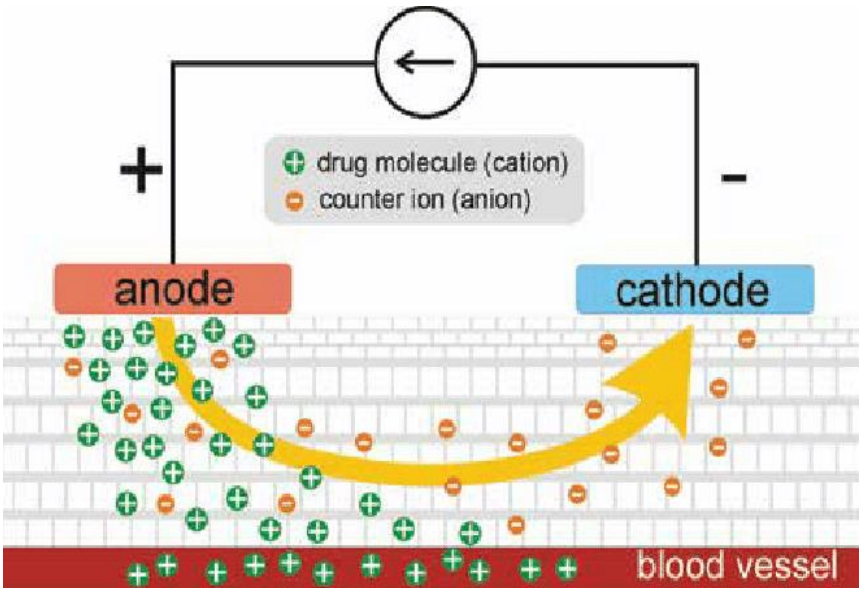

Fig 1.2. Iontophoresis technology.

Subramony JA, Sharma A, Phipps J. Microprocessor controlled transdermal drug delivery. Int. J. Pharm., 317, 1-6 (2006).

IP technology's mechanism relies on electrorepulsion and electroosmosis [50]. Electrorepulsion involves the migration of either positive- or negatively charged molecules into the skin after applying the anodal or the cathodal electrodes, respectively [50,51]. The density and the application time of the current and the exposed area of the skin surface can be modulated to enhance the magnitude of the drugs' migration through the skin barrier [47]. On the other hand, the negative charge of the human skin under normal physiological conditions allows for electroosmosis, which involves the convective movement of the solvent by the electric current [52,53]. Accordingly, the applied current of IP can facilitate the migration of the positively charged molecules from the anode to the cathode via an electroosmotic mechanism [52]. Moreover, it has been demonstrated recently that IP acts through opening the intercellular space [54]. After applying the electric field on the skin, the downregulation of connexin 43 and the depolymerization of F-actin resulted in the cleavage of both gap and tight junctions, respectively [54]. As a result, these led to attenuation between the cells and the creation of an intercellular transport shunt which eases the migration of molecules across the skin barrier. Taken together, the weak electricity of IP provides a driving force and activates an intercellular signaling pathway that cooperatively favors the permeation of biological macromolecules across skin barriers [54].

1.5. Application of iontophoresis

Recently, the transdermal delivery of various biological macromolecular drugs has been achieved using IP without needing a drug carrier [16]. Kigasawa et al. investigated IP technology's efficiency in delivering a non-formulated small interfering RNA (siRNA) intradermally for treating atopic dermatitis [55]. The authors found that the fluorescent signal of the labeled siRNA was distributed homogenously through the epidermal layer and up to the dermal junction after applying IP. Additionally, significant suppression in the interleukin (IL)-10 mRNA expression level related to the lesions of atopic dermatitis was obtained.

Accordingly, these results proved that IP-mediated delivery of non-formulated siRNA can contribute to treating atopic dermatitis patients. Moreover, IP technology successfully delivered antibody tumor necrosis factor (TNF)-α drug etanercept into the skin. Consequently, therapeutic efficiency was obtained against imiquimod-induced psoriasis [56]. Fukuta et al. found that following the use of IP, the fluorescent signal of the antibody was distributed deeply through the epidermal and dermal layers up to 1mm. After several doses of IP-mediated delivery of TNF-α drug etanercept on the psoriatic model in rats, a significant reduction by 50% in the IL-6 messenger RNA (mRNA) expression level was obtained, in addition to the suppression of epidermal hyperplasia. Furthermore, the authors demonstrated that the etanercept showed a great therapeutic effect after using IP technology compared to the s.c injection, which showed a low effect.

IP technology in the delivery of biological macromolecules is not only limited to inflammatory skin diseases, such as atopic dermatitis and psoriasis but also has been used for skin cancer. Cytosine-phosphate-guanosine oligodeoxynucleotides (CpG-ODNs) are single-stranded, short, synthetic DNA molecules that act as cancer immunotherapy [57,58]. Kigasawa et al. have demonstrated that IP-administered CpG-ODN succeeded in eliciting an immune response and a tumor regression in mice bearing melanoma [59]. This can prove the efficiency of non-invasive IP technology in cancer immunotherapy.

Finally, the application site of IP technology is not limited only to the skin; it can also be applied to other organs. Recently, Hasan et al. have demonstrated the success of IP in the delivery of naked siRNA into internal organs such as the liver and pancreas [60]. The authors found that the IP-mediated delivery of siRNA significantly suppressed heat shock protein 47 (HSP47) gene expression and ameliorated the pathological phenotypes of liver fibrosis.

Moreover, the author also demonstrated the significant knockdown of the pancreatic and duodenal homeobox-1 (Pdx-1) gene following the application of IP with anti-Pdx-1 siRNA onto the pancreas. In a broader sense, I can elucidate that IP technology has proven its ability to deliver various biological macromolecules through different organs for treating various diseases in a way that avoids systemic toxicity and non-specific distribution to other organs.

Although IP-mediated delivery of biological macromolecules showed great efficiency, it is still on the laboratory level. On the other hand, FDA has approved the non-invasive IP technology for the transdermal delivery of different small molecule drugs, such as fentanyl, lidocaine, and sumatriptan, to manage post-operative pain, induce local anesthesia and treat migraines, respectively [61]. To that end, I focused on utilizing IP technology for the transdermal delivery of different vaccines against the melanoma growth.

Chapter II

The Effect of Iontophoretic-Delivered Polyplex Vaccine on Melanoma Regression

Chapter II: The Effect of Iontophoretic-Delivered Polyplex Vaccine on Melanoma Regression

2.1. Introduction

Melanoma is the most serious type of skin cancer because of its aggressiveness and prognostic challenges [62,63]. Melanoma accounts for over 80% of skin cancer deaths [64,65], and cases are commonly rising in fair-skinned individuals in Europe, North America and other parts of the world [63]. Despite significant progress in understanding the pathogenesis of melanoma, incidence and mortality rates of this malignant type of cancer continue to rise globally [63]. It has been reported that melanoma accounts for 1.7% of global cancer diagnoses and is the 5th most prevalent cancer in the USA [64]. Various therapeutic approaches to treating melanoma are available, including surgery, radiation, chemotherapy and, recently, immunotherapy and targeted therapy [66]. According to the Cancer Treatment Centers of America® (CTCA), melanoma paved the way for the use of immunotherapy and targeted treatment strategies to stimulate the immune system to prohibit the deception of tumor cells. Consequently, prognosis, and morbidity and mortality rates are expected to substantially improve, not only in melanoma but in other types of cancers as well [67]. Melanoma vaccine therapy is currently under clinical investigation for treating stage III melanoma according to the declaration of National Cancer Institute (NCI).

Vaccines offer promising therapeutic strategies among prevailing infectious diseases [68-70]. In the last 2 decades, the scientific community has benefited from host immune surveillance in developing cancer vaccines [68,69]. Nowadays, cancer vaccines are recognized as a serious breakthrough for inducing tumor regression [69]. Further, cancer vaccines have shown promising results in pre-clinical studies and human clinical trials [71]. However, a cancer vaccine should ideally prevent the disease from occurring, while cancer

vaccines have typically relied on therapeutic effects against an established tumor [68,70,72,73]. The fundamental mechanism of action of cancer vaccines depends on activation of both antigen presenting cells (APCs), such as dendritic cells (DCs) and macrophages, with the aim of capturing antigens provided by the vaccines [68,69,71,74,75]. These activated APCs can then control the differentiation of T cells by presenting the processed antigens [68,69,71,76]. Although there are various subpopulations of T cells, cytotoxic $CD8^+$ T cells are considered to be the most crucial type for eradication of tumor cells [68,69,71,74,76,77]. The main goal of cancer vaccines is to induce tumor regression and establish a long-lasting protection via memory T cells [68,69,71,73,74].

Cancer vaccination research is aimed at developing prophylactic cancer vaccines that minimize the incidence rate and enhance the prognosis of cancers. Such efforts can positively reduce the economic burden, as well as morbidity and mortality rates [78-81]. There are currently 5 FDA-approved prophylactic vaccines to prevent cancers derived from hepatitis B virus (HBV) and human papilloma virus (HPV) [69,78,80,81]. The success in developing these vaccines offers prophylactic cancer vaccines as a promising strategy in the field of cancer research [78,82]. However, the global cancer burden related to viral etiology represents only <20% [78,80,83]. Therefore, various cancer research organizations, such as Cancer Research UK and NCI, have recognized the urgent need to develop successful prophylactic cancer vaccines for non-viral cancers, with the aim of reducing the malignancy burden worldwide [78,80,82,84]. Designing prophylactic cancer vaccines is a major challenge, in part due to the need to select safe and immunogenic tumor antigens that are considered appropriate for use [78,79,85]. Moreover, there are two categories of antigens, namely tumor specific antigens (TSAs), which are expressed specially in tumor tissues, and tumor associated antigens (TAAs), which are expressed in both tumor tissues and also at a low levels in normal tissues [69,78,86-88]. Although TSAs and TAAs are both prospective

targets for prophylactic vaccine design, TSAs are currently the most attractive for developing prophylactic vaccines because of their potent immunogenicity and low risk of the occurrence of immune tolerance and autoimmunity compared with TAAs [69,78,89].

Human $gp100_{25-33}$ antigen peptide (KVPRNQDWL) is a TAA that is significantly expressed in melanoma, as well as in normal melanocytes [90-92]. Despite its expression in normal melanocytes, it is the most commonly used antigen in the development of melanoma vaccines [91]. Previous studies have found that utilizing TAAs allows the immune response to cross-react with self-molecules that present on normal tissues, which can result in autoimmunity [80]. To overcome this issue, human $gp100_{25-33}$ antigen peptide has been combined with H-2Db complex, which belongs to a major histocompatibility complex (MHC) subgroup, with such modification leading to increased specificity for melanoma, as well as improvement in binding affinity to MHC I, stability and immunogenicity [90-93]. Indeed, the safety of the modified peptide on normal melanocytes allowed for its use as a tailored immunotherapy that is currently being investigated in clinical trials [70,94]. In this chapter, I relied on the safety point of this peptide for conducting a prophylactic study against non-viral cancer.

To achieve a more efficacious prophylactic vaccine, an appropriate adjuvant should be included [78,95]. It is known that addition of an adjuvant to the antigen can promote an immune response through various mechanisms that eventually lead to activation of both innate and adaptive immunity [78,80]. CpG-ODN acts on toll like receptor 9 (TLR9) to lead to a potent immune response via production of different inflammatory cytokines [89,96-98]. In addition, CpG-ODN has also been evaluated in combination with tumor antigens in various cancer immunotherapy studies [96,97].

In recent years, the skin has been considered as the most tailored target for eliciting an immune response [47,70,96,99]. The skin is fortified with different APCs that are located in both the epidermal and dermal layers [47,96,99]. Moreover, the most powerful APCs are the epidermal Langerhans cells (LCs), which exhibit the ability to expand their dendrites to the stratum corneum to capture various components of the vaccine, followed by activation of the immune system [37,70,96,99].

In this chapter, therefore, I evaluated the delivery of a prophylactic melanoma vaccine comprised of both the CpG-ODN adjuvant and an antigen peptide via skin using IP. I also evaluated the effectiveness of this vaccine on inhibiting melanoma growth *in vivo* compared with s.c injection. I investigated mRNA expression of various cytokines in different tissues, as well as infiltration of cytotoxic $CD8^+$ and $CD4^+$ T cells in the tumor tissue. Finally, I evaluated the therapeutic effect of this vaccine for reducing tumor growth in mice bearing melanoma.

2.2. Materials and Methods

2.2.1. Materials

CpG-ODN (ODN-1826 sequence: 5′-TCCATGACGTTCCTGACGTT-3′) and Sulfo-Cyanine3 (Cy3)-labeled CpG-ODN were purchased from Hokkaido System Science Co., Ltd., (Hokkaido, Japan). Human $gp100_{25–33}$ antigen peptide modified with tetra-arginine moieties (KVPRNQDWL-RRRR) and Fluorescein isothiocyanate (FITC)-labeled KVPRNQDWL-RRRR were synthesized by Peptide Institute, Inc. (Osaka, Japan). Optimal cutting temperature (OCT) compound, dako fluorescence mounting medium and Cellstain® DAPI Solution (4', 6-Diamidino-2-phenylindole, dihydrochloride) were obtained from Sakura Finetek (Tokyo, Japan), Agilent (Santa Clara, CA 95051, USA) and Fujifilm Wako Pure Chemical Corporation (Dojindo, Osaka, Japan), respectively. An Ag-AgCl electrode was purchased from 3 M Health Care (Minneapolis, MN, USA). ISOGEN with Spin Column RNA extraction reagent was purchased from Nippon Gene Co., Ltd., (Tokyo, Japan). All primers were purchased from Eurofins Genomics (Tokyo, Japan) and their sequences are shown in **Table 2.1**. PrimeScript™ RT Master Mix (Perfect Real Time) and TB Green® Premix Ex Taq™ II (Tli RNaseH Plus) were purchased from Takara Bio (Shiga, Japan). Bovine serum albumin (BSA) was purchased from Merck (Tokyo, Japan). Rabbit anti-mouse CD4, CD8 and Quantikine Enzyme-linked immunosorbent assay (Elisa) Kit (MIF00, R&D Systems) were obtained from Funakoshi Co., Ltd., (Tokyo, Japan). Goat anti-rabbit IgG H&L (Alexa Fluor® 488) was purchased from Abcam (ab150077, Tokyo, Japan). All other reagents used in this study were of the highest grade obtainable.

Table 2.1. Primer sequences used for reverse transcription polymerase chain reaction (RT-PCR).

Gene	Forward (5′ to 3′)	Reverse (5′ to 3′)
GAPDH (mouse)	AGGTCGGTGTGAACGGATTTG	GGGGTCGTTGATGGCAACA
IFN-γ (mouse)	ACAGCAAGGCGAAAAAGGATG	TGGTGGACCACTCGGATGA
TNF-α (mouse)	CAGGCGGTGCCTATGTCTC	CGATCACCCCGAAGTTCAGTAG
IL-6 (mouse)	CTGCAAGAGACTTCCATCCAG	AGTGGTATAGACAGGTCTGTTGG
IL-12b (mouse)	CTGGAGCACTCCCCATTCCTA	GCAGACATTCCCGCCTTTG

2.2.2. Animal and tumor cells

Male C57BL/6J mice (5 weeks old) were obtained from Japan SLC, Inc. (Shizuoka, Japan). B16F1 murine melanoma cells (Dainippon Sumitomo Pharma Biomedical Co., Ltd., Osaka, Japan) were cultured in Dulbecco's modified Eagle's medium (DMEM) containing both 10% fetal bovine serum (FBS) and 1% (v/v) antibiotics penicillin/streptomycin (100 U/ml), and incubated at 37°C in 5% CO2 atmosphere. All animal experiments were performed in accordance with the guidelines for care and use of experimental animals approved by the Animal and Ethics Review Committee of Tokushima University.

2.2.3. Preparation of polyplex nanoparticles

Polyplex nanoparticles were prepared according to a previous report [100]. First, 3.54 μl (8.91 μg) of positively-charged human $gp100_{25–33}$ antigen peptide (KVPRNQDWL-RRRR) (2.52 mg/ml) was diluted with RNase-free water to a total volume of 34.2 μl. Then, a 15.8 μl (10 μg) solution of negatively-charged CpG-ODN (0.63 mg/ml) was slowly added to the above diluted antigen peptide solution, and mixed gently with a micropipette, to yield a

final volume of 50 µl. The mixture was then allowed to incubate for 20 min at room temperature to facilitate self-assembly of the polyelectrolytes. The N/P ratio of the antigen peptide to CpG-ODN was optimized to prevent any reduction in the surface charge of the polyplex and also to obtain a small particle size. Particle size, zeta-potential, and polydispersity index (PDI) were measured with a Zetasizer Nano ZS (Malvern Instruments, Worcestershire, UK). Fluorescent-labeled polyplex nanoparticles were prepared in a similar way via gentle mixing of both FITC- labeled antigen peptide and Cy3- labeled CpG-ODN.

2.2.4. Iontophoresis of fluorescent-labeled polyplex nanoparticles

IP was carried out in mice according to our previous report with some modulations [60]. Briefly, mice were anesthetized by intraperitoneal injection of chloral hydrate (400 mg/kg mouse) dissolved in phosphate buffer solution (PBS). Mice were then shaved to expose their dorsal skin for IP application. For the administration of fluorescent-labeled polyplexes, nonwoven fabric (1 cm^2) moistened with 100 µl of labeled polyplexes (20 µg Cy3-CpG-ODN and 21.62 µg FITC-labeled antigen peptide) was placed on the shaved dorsal skin, and another nonwoven fabric (1 cm^2) wetted with 100 µl of PBS was added 1 cm away. Each piece of nonwoven fabric containing either labeled polyplexes or PBS was connected to Ag-AgCl electrodes. The Ag-AgCl electrodes with nonwoven fabric containing labeled polyplexes or PBS were connected to the cathode and anode, respectively, of a power supply (TTI Ellebeau, Inc., model TCCR-3005, Tokyo, Japan). IP was performed with a fixed current of 0.34 mA/cm^2 for 1 h. Finally, mice were incubated for 3 h, followed by euthanization and excision of their skin for cross sectioning. Additionally, topical application (-IP) of fluorescent-labeled polyplexes was also performed for 1 h followed by 3 h incubation.

2.2.5. Effect of iontophoresis on intradermal distribution of fluorescent-labeled polyplexes

After 3 h of incubation following IP application, mice were euthanized and their skin was excised, embedded in OCT compound, and then frozen with dry ice/ethanol. The frozen skin sections were cut into 10 μm thick sections using a cryostat (CM3050S; Leica Biosystems, Tokyo, Japan). The 10 μm thick frozen sections were mounted onto matsunami (MAS)-coated glass slides with dako fluorescence mounting medium and stored in the dark until dry. Finally, a confocal laser scanning microscope (CLSM) (LSM700, Carl Zeiss, Jena, Germany) was utilized to observe the distribution of fluorescent-labeled polyplexes in the skin sections exposed to IP or topical application (-IP).

2.2.6. *In vivo* vaccination for prophylactic studies

Healthy male C57BL/6J mice (6 weeks old) were pre-immunized by a fixed volume (50 μl) of different vaccine formulations, which were administered via one of two routes, namely s.c injection or IP. These formulations included pre-immunization with either positively-charged human $gp100_{25–33}$ antigen peptide vaccine (KVPRNQDWL-RRRR) (8.91 μg/dose mouse) or polyplex vaccine containing electrostatically-combined antigen peptide (8.91 μg/dose mouse) and CpG-ODN (10 μg/dose mouse), as described above. IP administration was carried out at 0.17 mA/0.5cm^2 for 1 h. The anode acted as the active electrode for delivery of the positively-charged antigen peptide formulation, while the cathode acted as the active electrode for delivery of the negatively-charged polyplex formulation. Four groups of mice were vaccinated: i) antigen peptide s.c injection, ii) antigen peptide IP, iii) polyplex s.c injection and iv) polyplex IP. For each group, 5 doses were administered every 3 days for a total of 13 days. Five days after the last immunization dose, mice were subcutaneously challenged into their flank (site of IP/s.c application) with B16F1

cells (8×10^4 cells/mouse) suspended in PBS. Tumor diameters were measured every other day using a digital caliper according to the following equation: T_{vol} (mm^3) = length × $width^2$ × 0.5. Tumor volume in vaccinated mice was compared with that of the control group. Mice were euthanized on day 23 (polyplex groups) and day 22 (antigen peptide groups) after tumor cells inoculation. Tissues (skin, spleen, and tumor) of mice vaccinated with polyplexes (IP or s.c injection) were harvested and stored at -80°C for further analysis.

2.2.7. RNA extraction

Tissues (skin, spleen, and tumor) were weighed (45-90 mg) and subsequently homogenized in the presence of 1 ml of ISOGEN Lysis reagent using TissueRuptor II (QIAGEN). The homogenate was then incubated for 5 min at room temperature. Finally, total RNA was purified and extracted with ISOGEN with Spin Column RNA extraction reagent according to the manufacturer's instructions. Total RNA concentration and purity were measured with a Nanodrop 8000 (Thermo Fisher Scientific, DE, USA).

2.2.8. Quantitative analysis of mRNA expression levels of inflammatory cytokines in different tissues using RT-PCR

Complementary DNA (cDNA) was prepared from the reverse transcription of 2 μg of total RNA extract using PrimeScript™ RT Master Mix and a MJ Mini Personal Thermal Cycler (BioRad Laboratories, Hercules, CA). The reverse transcription reaction was conducted at 37°C for 15 min, while inactivation of reverse transcriptase was conducted at 85°C for 5 min. RT-PCR analysis was performed using TB Green™ Premix Ex Taq™ II and a Thermal Cycler Dice Real Time System III (Takara Bio). For analysis of the mRNA expression levels of interferon (IFN)-γ, TNF-α, IL-6, IL-12b and glyceraldehyde-3-phosphate dehydrogenase (GAPDH), cDNA was denatured at 95°C for 30 s, followed by 40 cycles of

95°C for 5 s and 60°C for 30 s for amplification. The sequences of the primers used are shown in **Table 1.** The mRNA expression levels of IFN-γ, TNF-α, IL-6 and IL-12b were calculated using the $2^{-\Delta\Delta Ct}$ method by normalization relative to GAPDH mRNA.

2.2.9. Immunohistochemistry analysis of infiltrated $CD8^+$ and $CD4^+$ T cells in tumor tissue after pre-immunization with iontophoretic-administered polyplexes

At day 23 post tumor cells inoculation in pre-immunized mice, the tumor tissue was collected, embedded in OCT and stored at -80°C, as described above. Then, frozen blocks of tumor tissue were cut into 10 μm thick sections using a cryostat (CM3050S; Leica Biosystems, Tokyo, Japan), and subsequently immunostained for both $CD8^+$ and $CD4^+$ T cells. The tumor sections were washed first by PBS, followed by blocking with 1.5 % BSA dissolved in PBS containing 0.1% Tween-20 for 15 min at room temperature. Tumor sections were incubated with the diluted rabbit anti-mouse CD8 and CD4 primary antibodies separately for 18 h at 4°C. Then, the tumor sections were incubated with the diluted Alexa 488-labeled goat anti-rabbit IgG for 1 h at room temperature. DAPI was used for staining the nucleus. Finally, tumor sections were mounted with dako fluorescence mounting medium and left to dry. The tumor sections were observed using CLSM (LSM700, Carl Zeiss, Jena, Germany).

2.2.10. *In vivo* vaccination for long-term prophylactic study

The regimen of IP-administered polyplex vaccine was conducted in the same manner as described above, with the only difference being that mice were subcutaneously challenged into their flank with B16F1 cells at 2 months from the last immunization dose. Tumor volume in vaccinated group was compared with that of the non-vaccinated group. Mice were euthanized on day 21 after tumor cells inoculation.

2.2.11. *In vivo* vaccination by polyplexes for therapeutic studies

Male C57BL/6J mice (6 weeks old) were subcutaneously challenged into their flank with B16F1 cells (5×10^5 cells/mouse) suspended in PBS (day 0). Treatment with polyplex vaccine was initiated on day 3 after tumor cells inoculation. Five doses were administered on days 3, 6, 9, 12 and 15. Polyplexes were administered via one of two routes, namely IP (above the tumor site) or s.c injection (near the tumor site). The conditions for IP application and the doses of the polyplexes were the same as those described previously for the *in vivo* prophylactic studies. Tumor volume was determined as previously described, and mice were euthanized on day 21 after tumor cells inoculation. Skin, spleen and tumor tissues were harvested and stored at -80°C for further analysis.

2.2.12. ELISA

Male C57BL/6J mice (6 weeks old) were subcutaneously challenged into their flank with B16F1 cells (2×10^4 cells/mouse) (day 0). Therapeutic polyplexes were administered via one of two routes, namely IP (above the tumor site) or s.c injection (near the tumor site) as mentioned above. Blood was collected on days 4, 7, 8, and 21 after tumor cells inoculation. Blood samples were stored at 4°C for 3 h followed by centrifugation (Tomy, MX-160, Tokyo, Japan) at 2490 g/30 min for separation of serum, which was stored at -80°C until assayed. Finally, serum IFN-γ levels were determined by sandwich ELISA using Quantikine kit (MIF00, R&D Systems).

2.2.13. Statistical analysis

One-way analysis of variance (ANOVA) with Tukey post-hoc test was used for evaluating statistical differences among 3 groups. Data are presented as mean ± standard deviation (S.D).

2.3. Results

2.3.1. Preparation of polyplex nanoparticles

Polyplex nanoparticles prepared at an N/P ratio of 1 have been shown to exhibit the smallest particle size (253.4 ± 3.8), as well as appropriate zeta potential (-40.4 ± 1.1), and a PDI of 0.29 ± 0.02, compared to polyplexes prepared at other N/P ratios which showed either large particle size as in N/P ratio of 0.5 or low zeta potential as in N/P ratio of 1.5 and 3 (**Table. 2.2**).

Table 2.2. Physicochemical properties of polyplex nanoparticles prepared at different N/P ratios.

	N/P (0.5)	N/P (1)	N/P (1.5)	N/P (3)
Particle size (nm)	327.6±5.62	253.4±3.8	254.23±3.97	264.37±7.38
Zeta potential (mV)	-35.96±0.21	-40.4±1.1	+0.61±0.01	+9.17±0.36
Polydispersity index	0.31±0.01	0.29±0.02	0.19±0.03	0.28±0.04

2.3.2. Iontophoresis of fluorescent-labeled polyplex nanoparticles

To investigate the effectiveness of IP on the intradermal delivery of polyplex nanoparticles, FITC-labeled antigen peptide (green signal) and Cy3-labeled CpG-ODN adjuvant (red signal) were gently mixed to produce fluorescent-labeled polyplexes. IP was applied for 1 h, followed by 3 h incubation, and then observation of the distribution of fluorescent-labeled polyplexes in the skin sections. Fluorescence was not detected in the non-treated healthy skin - IP (**Fig. 2.3.a**). As shown in **Fig. 2.3.b**, following topical application (-IP) of fluorescent-labeled polyplexes, the green fluorescence of FITC-labeled antigen peptide was barely noticeable on the surface of the skin, while the red fluorescence of the Cy3-

labeled CpG-ODN adjuvant was slightly distinct. On the other hand, after IP application of fluorescent-labeled polyplexes, both the green fluorescence of FITC-labeled antigen peptide and the red fluorescence of Cy3-labeled CpG-ODN adjuvant showed distinct penetration into the skin to a depth of about 20 μm (**Fig. 2.3.c**). Co-localization of both green fluorescence and red fluorescence appeared as yellow fluorescence.

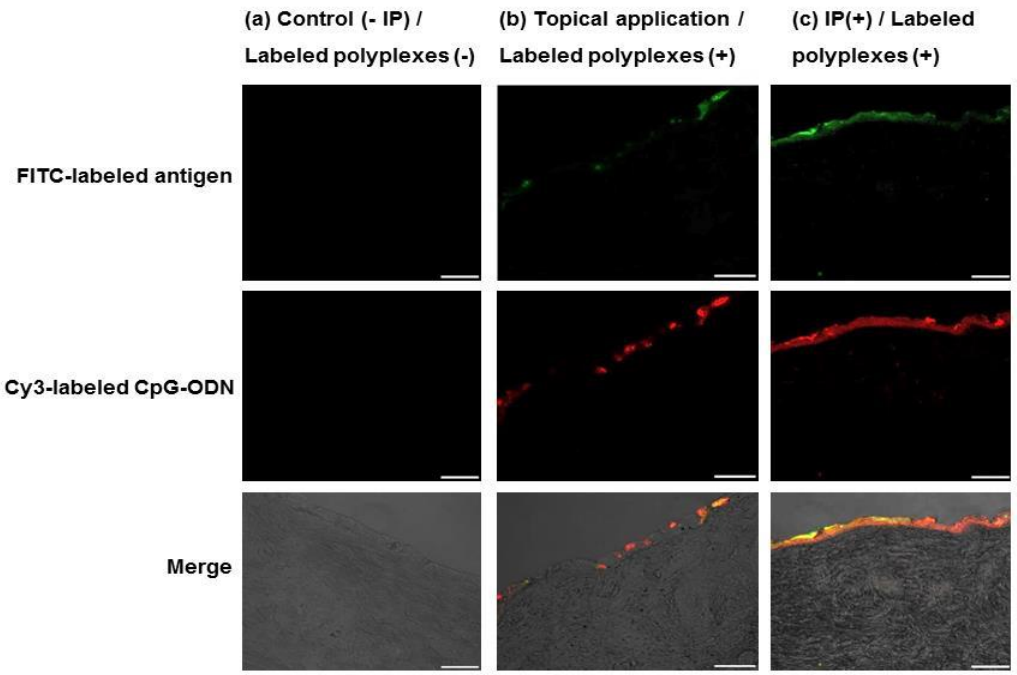

Fig 2.3. Distribution of fluorescent-labeled polyplexes in skin tissue after IP application.

Labeled polyplexes were prepared by gently mixing FITC-labeled human $gp100_{25\text{-}33}$ (KVPRNQDWL-RRRR) antigen peptide (green) with Cy3-labeled CpG-ODN (red). Cross sections of hairless frozen skin mice (10 μm) were prepared for observation with CLSM. (a) control group (-IP)/labeled polyplexes (-). (b) topical application, nonwoven fabric moistened with fluorescent-labeled polyplex solution and attached to the dorsal skin of mice for 1 h followed by 3 h incubation. (c) intradermal distribution of fluorescent-labeled polyplexes after IP application (0.34 mA/cm^2, 1 h) followed by 3 h incubation. Merged images of phase contrast, FITC (human $gp100_{25\text{-}33}$ KVPRNQDWL-RRRR; green), and Cy3(CpG-ODN; red) are shown. Scale bars = 50 μm.

Surprisingly, I found a very faint red fluorescence for Cy3-labeled CpG-ODN adjuvant distributed through the epidermal layer at depths beyond 50 μm, while FITC-labeled antigen peptide was distributed to a depth of only about 20 μm (**Fig. 2.4**).

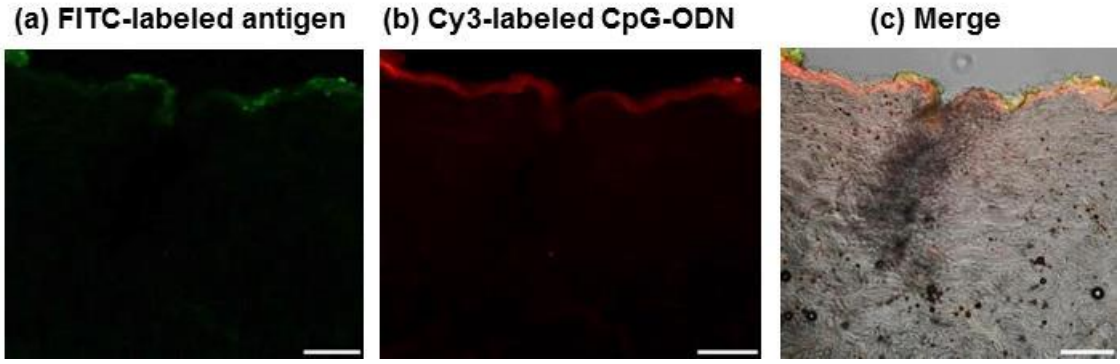

Fig 2.4. Deep penetration of Cy3-labeled CpG-ODN in skin tissue after IP application.

Distribution of fluorescent-labeled polyplexes in skin tissue after IP application (0.34 mA/cm^2, 1 h) followed by 3 h incubation. (a) FITC-labeled antigen showed distribution to a depth about 20 μm. (b) Cy3-labeled CpG-ODN showed distribution at depths beyond 50 μm. (c) merge. Merged images of phase contrast, FITC (human $gp100_{25\text{-}33}$ KVPRNQDWL-RRRR; green), and Cy3(CpG-ODN; red) are shown. Scale bars = 50 μm.

2.3.3. Effect of iontophoretic-administered prophylactic polyplex vaccine on melanoma inhibition

In this study, I first evaluated the effect of using human $gp100_{25–33}$ antigen peptide (KVPRNQDWL-RRRR) alone as a preventive vaccine in stimulating the immune system in tumor-free mice to delay the onset of melanoma, as well as to inhibit tumor growth. Tumor-free male C57BL/6J mice were vaccinated with antigen peptide via s.c injection or IP. Mice were pre-immunized with 5 doses of the antigen peptide, and after 5 days from the last immunization dose they were inoculated with B16F1 cells **(Fig. 2.5.a)**. As predicted, there was a slight reduction in tumor volume in the mice vaccinated by either both s.c injection and IP compared to non-vaccinated mice; however, this suppression was not significant (**Fig. 2.5.b**).

Hence, to enhance the efficiency of prophylactic antigen peptide vaccine, I inserted CpG-ODN adjuvant into the vaccine to produce polyplex nanoparticles. Next, I examined the potential prophylactic effect of polyplexes on production of immune cells in healthy mice to fight against melanoma growth. As shown in **Fig. 2.5.c**, there was a significant reduction in tumor volume after pre-immunization with the polyplex vaccine (both s.c injection and IP) compared to non-vaccinated mice, with an exception only at day 11 in the s.c.- vaccinated group, where a non-significant difference was observed compared to non-vaccinated mice (Tukey test). Also, the difference in tumor reduction between s.c.- and IP-vaccinated groups was not significant.

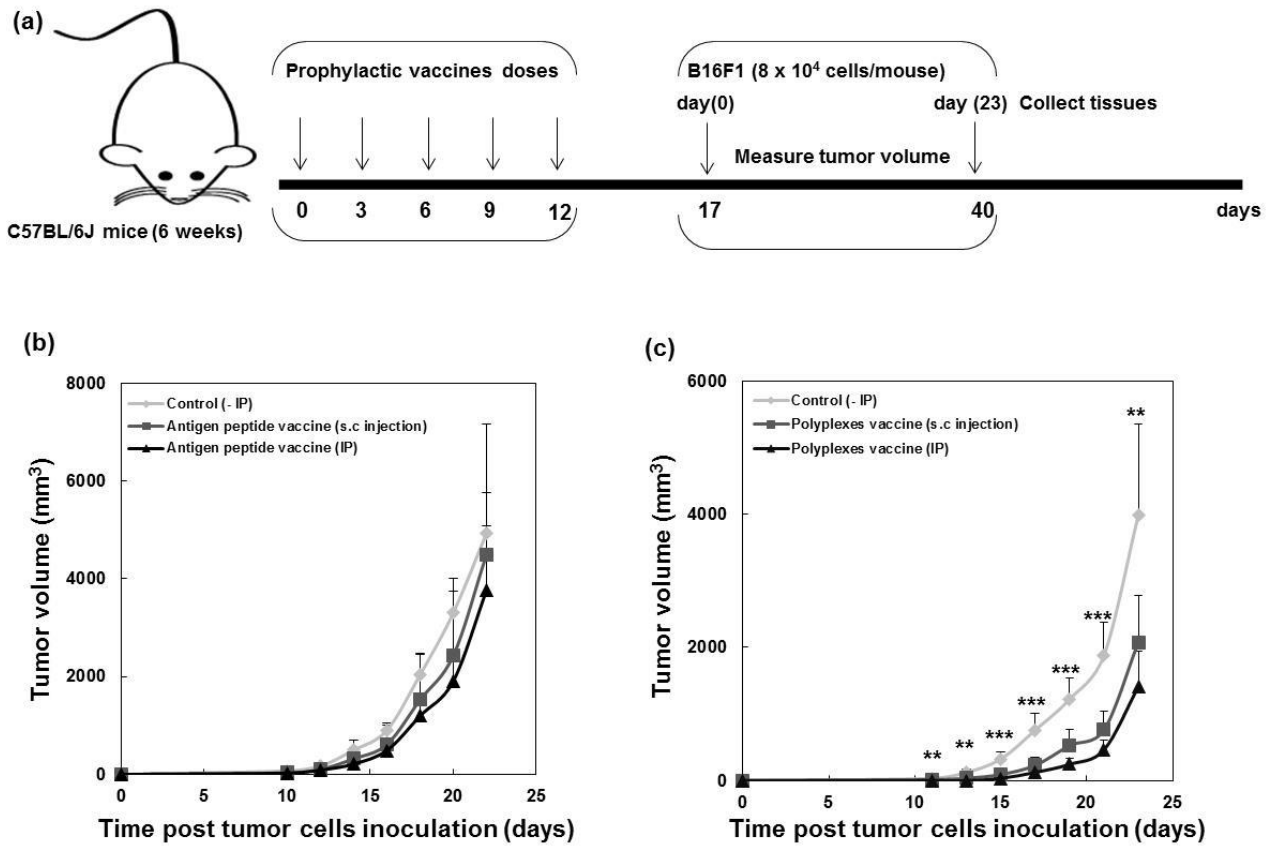

Fig 2.5. Effect of pre-immunization with prophylactic vaccines on tumor regression.

(a) schematic illustration of pre-immunization regimen with prophylactic vaccines against melanoma growth. (b) antigen peptide vaccine. (c) polyplex vaccine. Male C57BL/6J mice were pre-immunized by different routes (either s.c. injection or IP). Five doses were administered every 3 days. Then, 5 days after the last immunization dose, mice were subcutaneously inoculated with B16F1 cells (site of IP/s.c application). Tumor burden was measured every other day using a digital caliper. Values represent the mean ± SD ($n = 4$). Significant differences (**$P < 0.01$, ***$P < 0.001$) were found in groups of mice vaccinated with polyplex vaccine either by s.c. injection or IP, while there were no significant differences between groups vaccinated with antigen peptide vaccine (either by s.c. injection or IP) compared with the non-vaccinated group.

2.3.4. The role of cytokines production and infiltration of cytotoxic $CD8^+$ T cells in inhibiting melanoma growth after pre-immunization with iontophoretic-administered polyplex vaccine

To demonstrate the ability of polyplex vaccine delivered by IP to activate the immune system against tumor growth, I examined the mRNA expression levels of different cytokines, namely IFN-γ, TNF-α, IL-6 and IL-12b, in various tissues of IP-vaccinated mice compared with mice vaccinated by s.c. injection. Skin, spleen, and tumor tissues were collected at day 23 after tumor cells inoculation in pre-immunized mice (**Fig. 2.5.a**). Results revealed a significant elevation in mRNA expression levels of all analyzed cytokines in the skin tissue compared with the non-vaccinated group, except for IFN-γ and TNF-α in the s.c. injected group. The IP vaccinated group also showed a non-significant elevation in IL-12b which may be attributed to the difference in immune response among mice (**Fig. 2.6.a**). On the other hand, a significant elevation in mRNA expression levels was observed for all analyzed cytokines in the spleen tissue of vaccinated mice compared with non-vaccinated mice, except for TNF-α level in the s.c injected group (**Fig. 2.6.b**). Also, mRNA expression levels of all analyzed cytokines in the tumor tissue of vaccinated mice showed a significant elevation compared with non-vaccinated mice, except for TNF-α level in the s.c injected group and IL-12b level in the IP-vaccinated group (**Fig. 2.6.c**). There was a non-significant difference in mRNA expression levels of all examined cytokines in all tissues in the s.c injected group compared with the IP vaccinated group, with the only exceptions being in the skin and tumor tissues, where IL-6 and IL-12b showed significant differences, respectively. Moreover, levels of IFN-γ and IL-12b were the highest compared to other cytokines in all examined tissues. Higher levels of all cytokines were present in the tumor tissue compared with the skin and spleen tissues (**Fig. 2.6.c**).

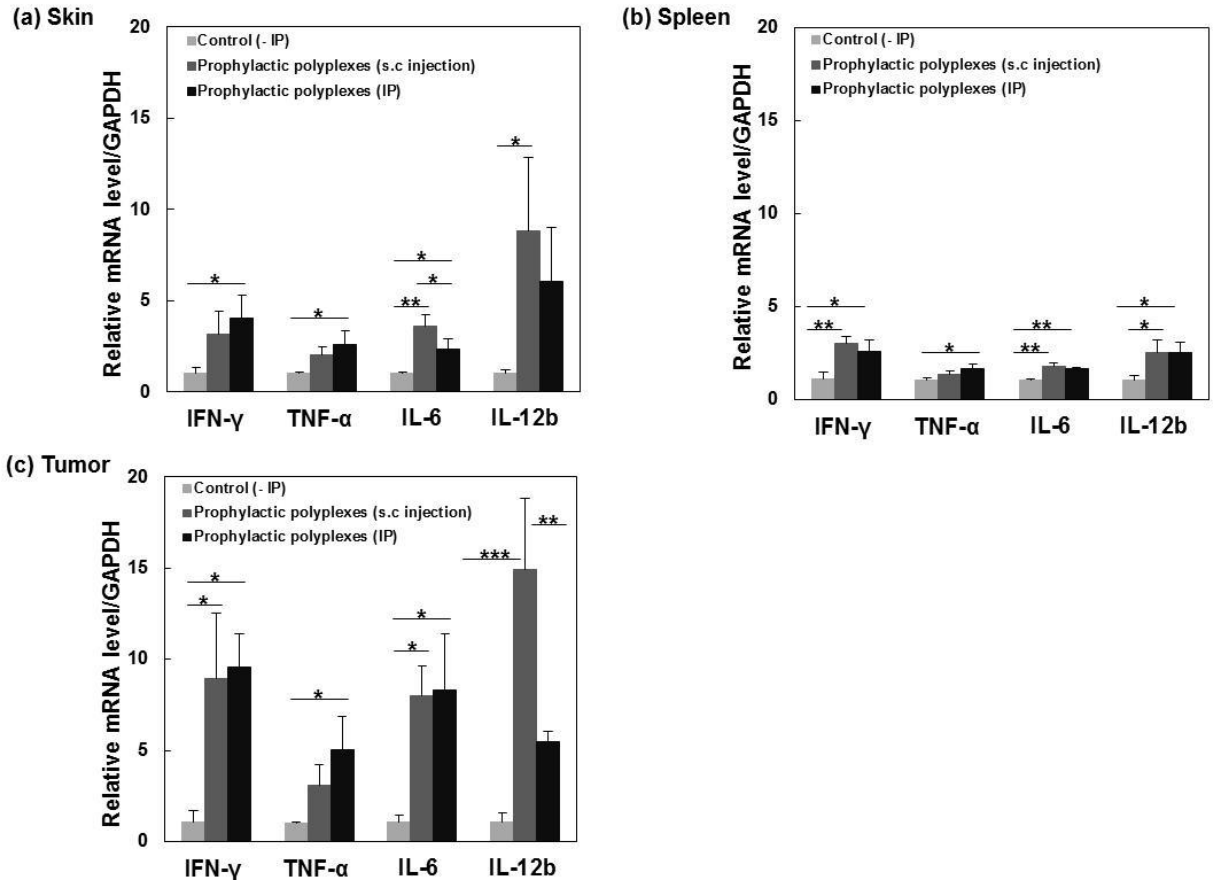

Fig 2.6. Quantitative analysis of mRNA expression levels of inflammatory cytokines in different tissues of prophylactic vaccinated mice.

(a) skin, (b) spleen, and (c) tumor tissues. Male C57BL/6J mice were pre-immunized with the polyplex vaccine via IP or s.c. injection (the site of tumor cells inoculation) as mentioned in **(Fig. 2.5.a).** At day 23 after tumor cells inoculation, mice were euthanized and tissues were collected. Quantitative evaluation of mRNA expression levels of different cytokines, namely IFN-γ, TNF-α, IL-6 and IL-12b, using RT-PCR was performed. Data are mean ± S.D. ($n = 3$). (*$P < 0.05$, **$P < 0.01$, ***$P < 0.001$).

Based on these findings, I evaluated the infiltration of both cytotoxic $CD8^+$ and $CD4^+$ T cells in tumor tissue after pre-immunization of healthy mice with IP-administered polyplex vaccine. I performed immunohistochemical analysis to detect $CD8^+$ and $CD4^+$ T cells in tumor tissue collected on day 23 post tumor cells inoculation in pre-immunized mice. Results showed a significant infiltration of both cytotoxic $CD8^+$ and $CD4^+$ T cells (green signals) in the tumor tissue compared with non-vaccinated mice (**Figs. 2.7**).

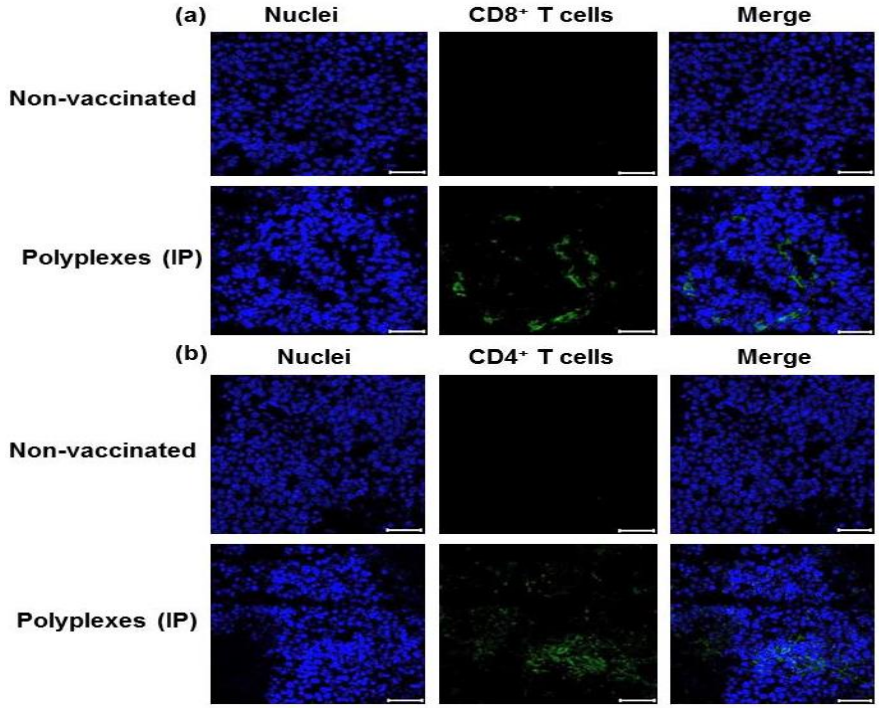

Fig 2.7. Immunohistochemical detection of infiltrated cytotoxic $CD8^+$ and $CD4^+$ T cells in tumor tissue.

Tumor tissues were collected on day 23 after tumor cells inoculation in mice pre-immunized with the polyplex vaccine by IP (the site of tumor cells inoculation). (a) infiltrated $CD8^+$ T cells. (b) infiltrated $CD4^+$ T cells. $CD8^+$ and $CD4^+$ T cells are represented by the green (Alexa 488) fluorescence. Nuclei are stained blue (DAPI). Scale bars = 50 μm.

2.3.5. Effect of long-lasting immunity on melanoma regression after pre-immunization with iontophoretic-administered polyplex vaccine

To evaluate the long-term efficacy of the IP-administered prophylactic polyplex vaccine, healthy mice were pre-immunized as previously described (**Fig. 2.5.a**) and then subcutaneously inoculated with B16F1 cells 2 months after the last immunization dose. I found that 3 of 4 vaccinated mice (**Fig. 2.8.b**) exhibited a reduction in tumor volume compared to non-vaccinated mice (**Fig. 2.8.a**).

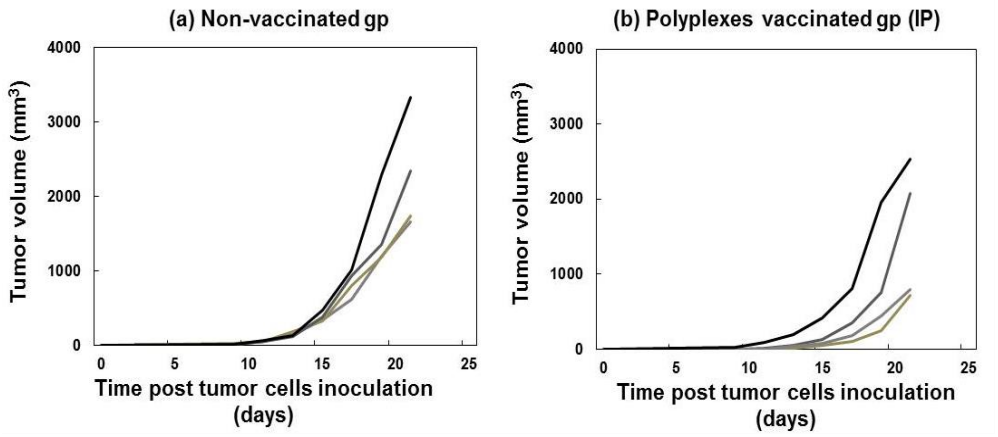

Fig 2.8. Influence of the long-term prophylactic effect of polyplex vaccine on tumor regression.

Male C57BL/6J mice were pre-immunized with the polyplex vaccine using IP. Five doses of the polyplex vaccine were administered to mice as shown in **(Fig. 2.5.a).** Two months later, mice were subcutaneously inoculated with B16F1 cells (site of IP application). (a) non-vaccinated group. (b) polyplexes vaccinated group (IP). Each line represents tumor volume of an individual mouse. Each group / (n= 4).

2.3.6. Effect of iontophoretic-delivered therapeutic polyplex vaccine on cytokines production and melanoma inhibition

Next, I examined the therapeutic effect of polyplex vaccine on tumor regression in mice bearing melanoma. Previously, the therapeutic efficacy of both an antigen peptide-loaded nanogel and free CpG-ODN adjuvant separately on reducing tumor burden in a melanoma model using IP was determined [70,96]. Despite both separately resulted in a significant reduction in tumor volume, their effects were not potent. Thus, I sought to combine the antigen peptide and the adjuvant in the form of a polyplex to enhance their therapeutic effects. I found a significant and potent reduction in tumor volume in mice bearing melanoma treated with either both s.c- and IP-administered polyplex vaccine compared to non-vaccinated group (**Fig. 2.9**). Also, there was a non-significant difference between s.c- and IP-treated groups.

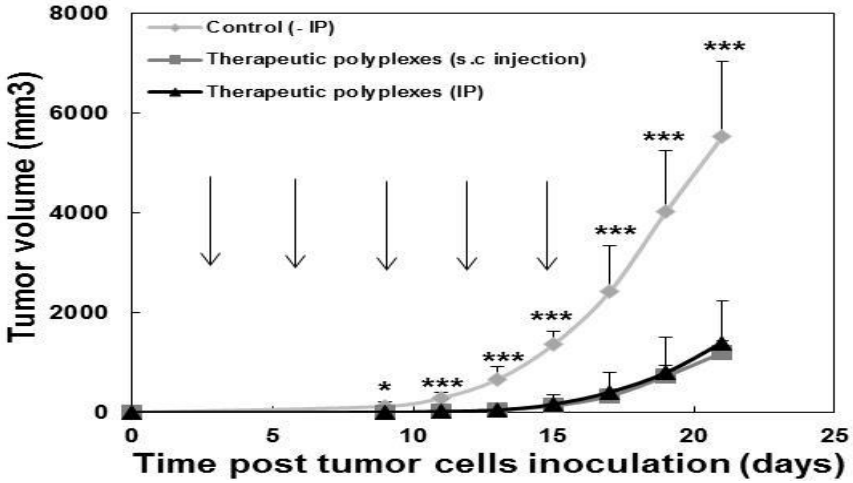

Fig 2.9. Anti-tumor effect of the therapeutic polyplex vaccine in mice bearing melanoma.

Male C57BL/6J mice were subcutaneously challenged into their flank with B16F1 cells (day 0). The therapeutic polyplex vaccine was administered via IP (above the tumor site) or s.c. injection (near the tumor site) on days 3, 6, 9, 12 and 15 (indicated by arrows). Values represent the mean ± SD (n = 4). Significant differences ($*P < 0.05$, $***P < 0.001$) were noted between the vaccinated and non-vaccinated groups.

Moreover, to confirm the induction of immunity, I determined mRNA expression levels of various cytokines in skin, spleen and tumor tissues. A significant elevation in cytokine levels was found in the skin tissue of vaccinated mice compared with non-vaccinated mice (**Fig. 2.10.a**), with the exception of IL-12b in IP-vaccinated group and IFN-γ and TNF-α in s.c-vaccinated group. Also, there was a significant elevation in the level of cytokines in the spleen (**Fig. 2.10.b**), with the exception of IFN-γ and IL-12b levels in IP- and s.c-vaccinated groups, respectively. Finally, cytokine levels significantly increased in the tumor tissue (**Fig. 2.10.c**), with the exception of TNF-α and IL-12b levels in s.c- and IP-vaccinated groups, respectively. There was a non-significant difference in mRNA expression levels of all examined cytokines in all tissues in the s.c injected group compared with the IP vaccinated group, with the only exception being in the tumor tissue, where IL-6 showed a significant difference. Furthermore, all examined cytokines showed the highest expression levels in tumor tissue compared with the skin and spleen tissues.

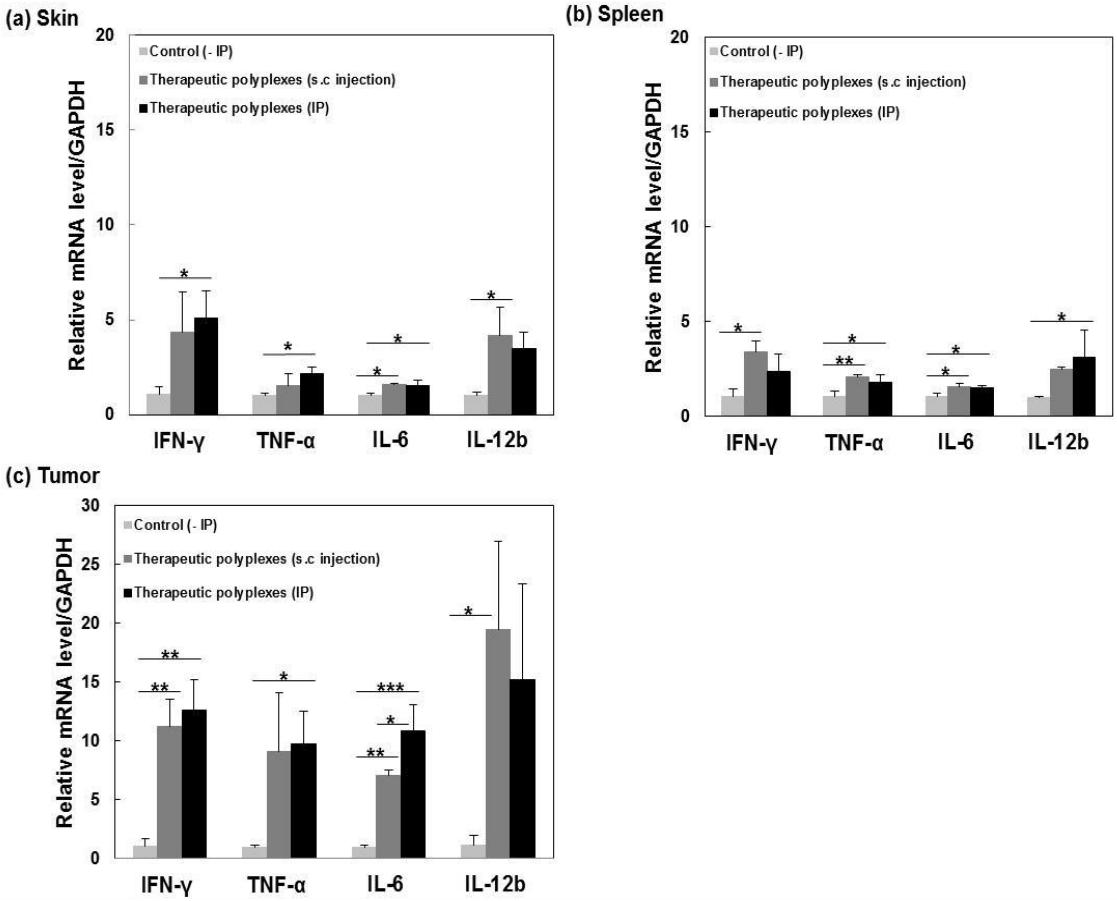

Fig 2.10. Quantitative analysis of mRNA expression levels of inflammatory cytokines in different tissues of mice bearing melanoma treated with the polyplex vaccine.

(a) skin, (b) spleen, and (c) tumor tissues. Mice bearing melanoma were treated with the polyplex vaccine via IP (above the tumor site) or s.c. injection (near the tumor site). At day 21 after tumor cells inoculation, mice were euthanized and tissues were collected. Quantitative evaluation of mRNA expression levels of different cytokines, namely IFN-γ, TNF-α, IL-6 and IL-12b, using RT-PCR was performed. Data are mean ± S.D. (n = 3). (*P < 0.05, **P < 0.01, ***P < 0.001).

2.3.7. Iontophoretic delivery of therapeutic polyplex vaccine enhanced systemic immunity

Finally, to confirm whether the local immune response mediated by the activated skin resident immune cells could gradually initiate a potent systemic immune response, I determined IFN-γ serum level. After subcutaneously inoculating mice with B16F1 cells (day 0), mice were subsequently treated with polyplex vaccine via one of two routes, namely IP or s.c. injection as mentioned above. IFN-γ serum levels were analyzed on days 4, 7, 8, and 21 post tumor cells inoculation. Results showed a significant elevation in IFN-γ serum levels on day 4 in both IP- and s.c- vaccinated groups compared to the control group **(Fig.2.11).** A gradual increase in IFN-γ serum levels was observed on day 7, which was non-significant in IP- and s.c- vaccinated groups compared to the control group. Moreover, there was a downregulation in IFN-γ serum levels on day 8 compared to days 4 and 7, but the level was still significantly elevated in both IP- and s.c- vaccinated groups compared to that of the control group (**Fig. 2.11**). Finally, at day 21 IFN-γ serum levels were nearly similar to the levels at day 8. Additionally, there was a non-significant difference between IP- and s.c-vaccinated groups in all days.

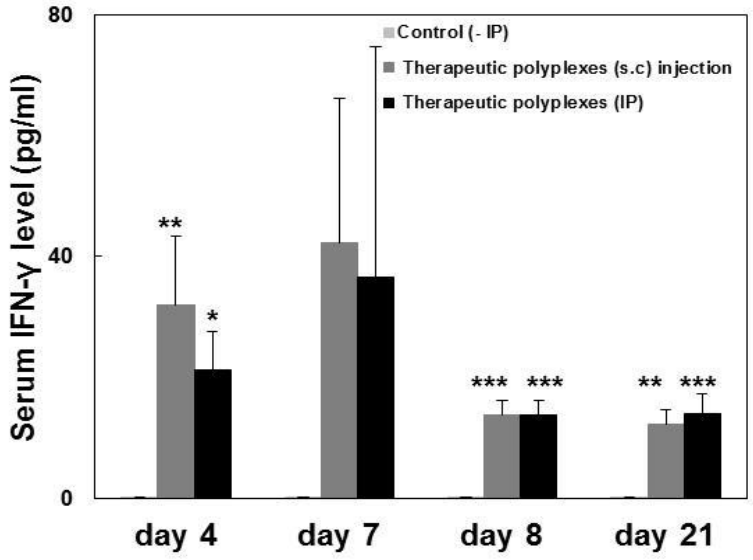

Fig 2.11. Detection of IFN-γ levels at different time intervals in the serum of mice bearing melanoma treated with the polyplex vaccine.

Male C57BL/6J mice were subcutaneously challenged into their flank with B16F1 cells (day 0). Then, mice were treated with the polyplex vaccine via IP (above the tumor site) or s.c. injection (near the tumor site). At days 4, 7, 8, and 21 post tumor cells inoculation, blood was withdrawn for determination of IFN-γ serum levels using ELISA kit. Data are mean ± S.D. ($n = 3$). (*$P < 0.05$, **$P < 0.01$, ***$P < 0.001$).

2.4. Discussion

Delivery of nucleic acid-based therapeutics via polyplex nanoparticles is considered a versatile strategy for a number of reasons, including the ability of polyplexes to condense nucleic acids into small nanoparticles, cost effectiveness, and ease of production [101-103]. In the present study, I prepared polyplex nanoparticles via electrostatic interactions between the negatively charged phosphate groups of the CpG-ODN adjuvant and the positively charged nitrogen atoms of human $gp100_{25–33}$ antigen peptide modified with tetra-arginine moieties (KVPRNQDWL-RRRR). The intracellular uptake of polyplex nanoparticles can be affected by particles size and surface charge [103]. Therefore, I prepared polyplex nanoparticles with different N/P ratios, ranging from 0.5–3, to obtain the most convenient particle size and zeta potential (**Table.2.2**). One of the main challenges with delivery of nucleic acids is the presence of extracellular and intracellular nuclease enzymes. To evade degradation of the polyplex nanoparticles by nuclease enzymes, I used a synthetic CpG-ODN adjuvant, which is characterized by the presence of a phosphorothioate backbone instead of the natural phosphodiester backbone. Results of a previous study demonstrated that the phosphorothioate motifs in CpG-ODN adjuvant provided resistance toward digestion by nuclease enzymes [104], which allowed for maintenance of the stability and the integrity of polyplex nanoparticles for cellular uptake.

Fluorescent-labeled polyplexes have shown accumulation within the epidermal layer after IP application (**Fig.2.3.c**). Such accumulation exposes the polyplexes to be captured by epidermal immune cells, mainly LCs, which distinguished by expanding their dendrites and so, can activate the immune system [70,96,105]. To that end, IP application resulted in intradermal delivery of fluorescent-labeled polyplexes prepared from hydrophilic macromolecules antigen peptide (M.W;1780) and CpG-ODN adjuvant (M.W;6363.01), as predicted based on our previous reports demonstrating transdermal delivery of hydrophilic

macromolecules using IP [56,60,70,96,106]. Surprisingly, I found a very faint red fluorescence for Cy3-labeled CpG-ODN adjuvant distributed through the epidermal layer at depths beyond 50 μm, which may attributed to free Cy3-labeled CpG-ODN adjuvant (**Fig. 2.4**). Additionally, I used the cathode as an active electrode because of the net negative charge of the polyplexes, which may have enhanced the permeation of the free Cy3-labeled CpG-ODN adjuvant through the skin by an electrorepulsion mechanism.

It is known that transcutaneous immunization depends on activation of skin-resident immune cells [96,107]. The skin is rich with a copious amount of APCs, such as LCs and dermal DCs [96,108]. Following activation of these cells by an invasive antigen or bacterial and viral elements, they migrate to draining lymph nodes (DLNs) [96,107,109]. Consequently, induction of mucosal or systemic immune response occurs via production of proinflammatory cytokines and differentiation of T cells by antigen presentation on the surface of the immune cells [68,96,110]. Human $gp100_{25–33}$ antigen peptide (KVPRNQDWL) derived from human melanoma exhibits the ability to cross-react with mice bearing melanoma [70]. Recently, this antigen peptide was investigated in clinical trials as a cancer immunotherapy [70,94]. In this study, using human $gp100_{25–33}$ antigen peptide (KVPRNQDWL-RRRR) alone as a preventive vaccine showed a non-significant effect against tumor growth (**Fig. 2.5.b**). The insufficiency of this prophylactic antigen peptide vaccine to suppress tumor volume or to even delay its onset is related to the weakness of the antigen immunogenicity [68,78,111]. Low immunogenicity is commonly mediated by numerous mechanisms, and is considered a major challenge in the development of vaccines, alongside the use of antigens alone, which cannot provoke proinflammatory cytokines, thereby resulting in low immunogenicity [68,111,112]. Results are consistent with previous studies [68,113] that used different antigens alone for vaccination, which also showed weak immunogenicity. As is common in vaccine development, to obtain a potent immunogenic

response, inclusion of an appropriate adjuvant is a crucial element. Adjuvants exhibit the ability to stimulate the immune system through various ways, such as by activation of the APCs to allow for antigen uptake, presenting antigens to T cells and B cells, and also by initiating innate immunity [78].

In a broader sense, after gathering the adjuvant with the antigen simultaneously, the formed polyplexes promoted activation of the immune system followed by reduction in tumor volume (**Fig.2.5.c**). It has been demonstrated that CpG-ODN adjuvant acts via TLR9, which is an intracellular receptor found in various immune cells, mainly LCs, dermal DCs, B cells and monocytes [96]. Stimulation of TLR9 leads to various immunostimulatory effects, including activation of innate immune cells, upregulation of proinflammatory cytokines, such as IL-6 and TNF-α, as well as production of Th1-type cytokines, such as IL-12, and IFN-γ [96,114]. Moreover, CpG-ODN adjuvant has been considered as the bridge between innate and adaptive immunity due to its ability to activate innate immune cells as well as APCs, which consequently engulf and process the antigen for presentation to naïve $CD4^+$ and $CD8^+$ T cells (adaptive immunity) [96,115]. Tumor-specific T cells are activated through binding of MHC–peptide complex to T cell receptors [69]. Following binding, the activated T cells differentiate into long lasting memory T cells and effector T cells [69]. Based on previous studies [68,69,72,116], $CD8^+$ T cells are proliferate and differentiate to yield cytotoxic T lymphocytes (CTLs), which are considered fatal cells for the tumor. Infiltration of cytotoxic tumor-specific $CD8^+$ T cells in the tumor, as well as $CD4^+$ T cells that control the differentiation of $CD8^+$ T cells and trigger the inflammatory microenvironment in the tumor and secretion of cytokines (mainly IFN-γ), are crucial elements for tumor regression [69,72,78,111,116].

Although tumor tissue is the primary target tissue for detection of mRNA expression levels of cytokine, I also examined these levels in the skin and spleen tissues for the following reasons. The skin is considered a crucial site for eliciting an immune response because it contains plenty of resident immune cells, including LCs, as well as keratinocytes, which represent the majority of the epidermis layer and exhibit the ability to elicit a potent immune response and secrete cytokines [96]. Moreover, spleen is considered as a second lymphoid organ. IP-delivered prophylactic polyplex vaccine activated the immune system and elicited substantial upregulation of cytokines (**Fig.2.6**), which contributed to cell-mediated immunity. Indeed, secretion of proinflammatory cytokines, such as TNF-α and IL-6, or Th-1 cytokines, such as IL-12b and IFN-γ, participate in activating both innate and adaptive immunity, which ultimately fights against melanoma growth [96,109,117,118]. IL-12b is a proinflammatory type I cytokine that is known for its crucial role in controlling adaptive cell-mediated immunity by eliciting the secretion of IFN-γ by APCs. In addition, IL-12b contributes to the differentiation of both $CD4^+$ and $CD8^+$ T cells by augmenting the secretion of IFN-γ [68,111,119]. Moreover, IFN-γ is considered one of the most important cytokines involved in killing tumor tissue owing to its ability to upregulate expression levels of MHC I and II molecules in the tumor tissue, which promote the detection of tumor cells by cytotoxic $CD8^+$ T cells to facilitate their clearance [68,69,116,120]. IFN-γ is also known to enhance the apoptosis process in tumor tissue, which inhibits angiogenesis and augments the differentiation of cytotoxic $CD8^+$ T cells [68]. Results confirmed the importance of IFN-γ and IL-12b secretion in the activation of cytotoxic $CD8^+$ T cells, which are mainly responsible for inhibition of tumor growth. Moreover, levels of IFN-γ and IL-12b were the highest compared to other cytokines in all examined tissues (**Fig.2.6**). On the other hand, the role of other proinflammatory cytokines, such as TNF-α and IL-6 should also be noted. TNF-α levels are highly correlated to cancer immunity by causing apoptosis and inflammation in addition to

contributing to differentiation and maturation of DCs, while IL-6 participates in the enhancement of $CD8^+$ T cell trafficking [68,69,116,121]. Infiltration of cytotoxic $CD8^+$ and $CD4^+$ T cells in the tumor microenvironment is critical for tumor regression. Prophylactic polyplex vaccine was able to generate immune cells, which showed expansion and infiltration into tumor tissue following challenge of pre-immunized mice with B16F1 cells (**Fig.2.7**), thus demonstrating the pivotal role of immune cells in tumor regression. After evaluating the long-term efficacy of the IP-administered prophylactic polyplex vaccine (**Fig. 2.8**), the result showed that the IP-administered polyplex vaccine may offer a prophylactic effect on the long-term. However, this long-term prophylactic effect needs for more improvement.

Also, I found a significant and potent reduction in tumor volume in mice bearing melanoma treated with either both IP- and s.c- administered polyplex vaccine (**Fig. 2.9**), confirming the pivotal role of the combination of the adjuvant and antigen on stimulating immunity. As noted earlier, this reduction in tumor volume can be attributed to cytokines secretion (**Fig.2.10**) in addition to infiltration of both cytotoxic $CD8^+$ and $CD4^+$ T cells in the tumor tissue. These results highlight the promising effect of iontophoretic delivery of a therapeutic polyplex vaccine in inhibiting melanoma growth via activation of the immune system and mediating the secretion of IFN-γ, which plays a pivotal role in tumor clearance through various mechanisms, including activation of cytotoxic $CD8^+$ T cells that are responsible for attacking the tumor.

Finally, the therapeutic polyplex vaccine was able to persistently stimulate the APCs, which participated in inducing a systemic immune response via secretion of IFN-γ cytokine (**Fig.2.11**) [96]. The immune system is known to take up to 3 days to prime the adaptive immune response, which is accomplished by low levels of cytokine secretion after the first immunization dose, followed by a peak in levels of cytokine secretion and the magnitude of the immune response after the second immunization dose, and then a subsequent plateau in cytokine levels [68]. Indeed, I found that IFN-γ serum levels were elevated after the first immunization dose on day 4 followed by tendency toward more elevation on day 7 which was non-significant in IP- and s.c- vaccinated groups compared to the control group (**Fig. 2.11**). Finally, on day 8, IFN-γ serum levels decreased and showed a steady state until day 21, which confirms the ability of therapeutic polyplexes delivered either by IP or s.c injection to induce and maintain a systemic immune response to fight against melanoma growth.

While there were no significant differences observed in either tumor regression or production of cytokines in the IP vaccinated group compared to the s.c. injected group, IP application is also suggested to be superior than s.c injection based on previous reports [55,96]. These reports demonstrated that about half of the applied amount of nucleic acid therapy was retained in the patch following IP application, while the full therapeutic dose was completely delivered following s.c. injection.

Interestingly, results of the present study suggest that the polyplex vaccine may be more powerful as a therapeutic vaccine than as a prophylactic vaccine, which may be due to two reasons. In particular, it is known that the action of prophylactic vaccines depends on memory immune cells, while therapeutic vaccines do not. In addition, Jason et al. reported that although memory immune cells can recognize a viral infection within a few hours, they start to proliferate and differentiate after about 3 days from the infection, thereby delaying the onset of activation in addition to exhibiting a slower rate of division than naïve cells [122]. Second, in my prophylactic vaccination protocol I inoculated the pre-immunized mice with a higher number of B16F1 cells than typically employed in other prophylactic vaccine studies that tend to inoculate mice with a very low number of tumor cells [72,79,111,116]. The above reasons may be responsible for the somewhat lower prophylactic effect of the polyplex vaccine compared to its therapeutic effect on reducing tumor volume. In any event, the polyplex vaccine did demonstrate both prophylactic and therapeutic effects against tumor growth.

2.5. Conclusion

In conclusion, the results of my study demonstrate that IP-administered polyplex vaccine was able to overcome the hurdles of the stratum corneum barrier and successfully deliver the vaccine into the epidermal layer for activation of LCs. Capability of IP-administered prophylactic polyplex vaccine to act as a safe immunogenic agent and stimulate immune cells to fight against melanoma growth. Moreover, *in vivo* tumor regression in pre-immunized mice was mediated via a series of events, including activation of APCs, elevation in mRNA expression levels of various cytokines, and also infiltration of cytotoxic $CD8^+$ and $CD4^+$ T cells in the tumor tissue. Additionally, the vaccine also exhibits a therapeutic effect against mice bearing melanoma.

Chapter III

Use of Iontophoresis Technology for Transdermal Delivery of a Minimal mRNA Vaccine as a Potential Melanoma Therapeutic

Chapter III: Use of Iontophoresis Technology for Transdermal Delivery of a Minimal mRNA Vaccine as a Potential Melanoma Therapeutic

3.1. Introduction

Vaccination is considered the most effective means for controlling and preventing the prevalence of infectious diseases [123]. In 2020, FDA approved two mRNA vaccines to combat COVID-19 pandemic [124]. In fact, the accelerated development of these COVID-19 mRNA vaccines relied on years of preclinical and clinical research aimed at enhancing the use of mRNA vaccines for cancer therapy [125]. As a result the COVID-19 pandemic, considerable attention has been focused on the development and use of mRNA vaccines and therapeutics for a wide variety of human diseases, including for heart diseases, autoimmune disorders, rare genetic diseases, human immunodeficiency virus (HIV), and has also provoked a breakthrough in the area of cancer vaccines [126-128]. Cancer vaccines mostly encode for different TAAs or TSAs aimed at stimulating cell-mediated immune responses, such as CTLs, which have the potential effect of attacking malignant cells [126,129].

Over the past decade, nucleic acid-based cancer vaccines, including mRNA vaccines and DNA vaccines, have been suggested as a promising platform over other conventional vaccines (e.g., peptide vaccines and viral vector-based vaccines) for various reasons, including improved safety, efficacy and the potential to elicit humoral- and cell-mediated immune responses [124,130]. However, nucleic acid-based vaccines are preferred over other traditional vaccines, while mRNA vaccines offer advantages over DNA vaccines [131]. Unlike DNA vaccines, mRNA vaccines lack the possibility for genomic integration, resulting in minimal concerns for gene disruption, mutagenesis and tumorgenesis

[130-132]. Moreover, mRNA vaccines are distinguished by their short half-lives and well-tolerated safety profile, as well as their rapid, high-yield, safe, and cost-effective production [123,125,129-132]. On the other hand, mRNA vaccines also have some disadvantages that limit their application, such as high molecular weights, instability, immunogenic properties, and insufficient *in vivo* delivery, which can lead to degradation of mRNA vaccines, inhibition of antigen expression, and consequently weak immune cells activation [126,129,132-134]. Hence, researchers and mRNA vaccine manufacturers are focusing their efforts on overcoming these difficulties via different approaches, such as designing various delivery vehicles for improving cellular uptake and cytoplasmic translation and improving the purification methods to eliminate double-stranded contamination that provokes innate immunity to result in mRNA vaccine degradation [126,130,135]. Furthermore, modifications in the backbone of mRNA vaccines, including the poly (A) tail, the 5' cap, un-translated regions, the sequence patterns in the open reading frame (ORF), and also incorporation of modified nucleotides, can contribute to overcoming the above-mentioned hurdles associated with mRNA vaccines [130].

In this chapter, a minimal mRNA based vaccine (M.W: 20,460) encoding TAA human gp100 $_{(25\text{-}33)}$ (KVPRNQDWL) as a potential melanoma therapeutic was prepared by introducing a short poly (A) tail 20-nt. Despite the resultant increase in length of the mRNA sequence, the poly (A) tail is crucial for protecting the mRNA vaccine from de-capping and degradation, as recent study has shown that shortening the poly (A) tail sequence could enhance the translation process in addition to simplifying the synthesis process [136]. While the negative charges and high molecular weights (10^5–10^6) of naked non-formulated mRNA vaccines can impair their intracellular uptake and efficacy, clinical trials have demonstrated success in inducing a potent anti-tumor immune response after intranodal, intradermal, and s.c injection of naked mRNA cancer vaccines [123,125,129,130]. However, intranodal

injection involves complicated procedures, and achieving high efficiency of injected naked mRNA vaccines is related to the high frequency of DCs in the DLNs [124,129,131]. Additionally, the intradermal route has been widely used for vaccine delivery [125,126,129]. In addition to the need for special training, intradermal injection can also increase the risk of undesirable side effects at the injection site, such as swelling, infection, erythema, and pain [56,70,96,124].

In the present study, I utilized two unique features related to IP: the first is the ability to deliver hydrophilic macromolecules via the stratum corneum of the skin; and the second is the potential to improve cellular uptake of negatively-charged hydrophilic macromolecules, as reported previously for siRNA [137,138]. In fact, IP and electroporation are used previously for the delivery of charged compounds like DNA, RNA and peptides. Despite the used voltage in electroporation is extremely higher and reach up to 100 Volt compared to IP (10 V or less), it has been reported that electroporation succeeded in the delivery of mRNA mouse zygotes and facilitated clustered regularly interspaced short palindromic repeats/CRISPR-associated protein 9 (CRISPR/Cas9)-based genome editing [139]. Also, electroporation has been shown to enhance the delivery efficiency of large, self-amplifying mRNA *in vivo*, upon measuring reporter gene expression and immunogenicity of genes encoding HIV envelope proteins [140]. Taken together, these reports proved that mRNA is stable electrically to the high voltage of electroporation. Herein, I investigated the potential effect of combining a chemically synthesized minimal mRNA vaccine with IP technology to enhance the transdermal delivery and the cellular uptake of naked non-formulated minimal mRNA vaccine as a potential melanoma therapeutic. I investigated the potential effect on reducing tumor volume in mice bearing melanoma and the mRNA expression levels of various cytokines by RT-PCR. Finally, I confirmed the stimulated immune

response through immunohistochemistry analysis for the infiltrated cytotoxic $CD8^+$ and $CD4^+$ T cells in the tumor tissue and systemically by detecting serum IFN-γ levels.

3.2. Materials and Methods

3.2.1. Materials

The FITC-labeled oligonucleotide GGAGCCACCATGAAGGTGCCCCGGAACCAGGACTGGCTGTGAAAAAAAAAAAA AAAAAAAAA (M.W:19,800) was purchased from Hokkaido System Science Co., Ltd., (Hokkaido, Japan). OCT compound, dako fluorescence mounting medium and Cellstain® DAPI Solution were obtained from Sakura Finetek (Tokyo, Japan), Agilent (Santa Clara, CA 95051, USA) and Fujifilm Wako Pure Chemical Corporation (Dojindo, Osaka, Japan), respectively. An Ag-AgCl electrode was purchased from 3M Health Care (Minneapolis, MN, USA). ISOGEN with Spin Column RNA extraction reagent was purchased from Nippon Gene Co., Ltd., (Tokyo, Japan). All primers were purchased from Eurofins Genomics (Tokyo, Japan) and their sequences are shown in **Table 2.1**. PrimeScript™ RT Master Mix and TB Green® Premix Ex Taq™ II were purchased from Takara Bio (Shiga, Japan). BSA was purchased from Merck (Tokyo, Japan). Rabbit anti-mouse CD4, CD8 and Quantikine Elisa Kit (MIF00, R&D Systems) were obtained from Funakoshi Co., Ltd., (Tokyo, Japan). Goat anti-rabbit IgG H&L (Alexa Fluor® 488) was purchased from Abcam (ab150077, Tokyo, Japan). All other reagents used in this study were of the highest grade available.

3.2.2. Animal and tumor cells

Male C57BL/6J mice (5 weeks old) were obtained from Japan SLC, Inc. (Shizuoka, Japan). DMEM containing both 10% FBS and 1% (v/v) antibiotics penicillin/streptomycin (100 U/ml) was used for culturing B16F1 murine melanoma cells (Dainippon Sumitomo Pharma Biomedical Co., Ltd., Osaka, Japan), and these cells were incubated at 37°C in 5% CO2 atmosphere. All animal protocols were evaluated and approved by the Animal and Ethics Review Committee of Tokushima University.

3.2.3. Iontophoresis technology for delivery of FITC-labeled oligonucleotide

FITC-labeled oligonucleotide (M.W:19,800) was used as a model of mRNA to investigate transdermal delivery by IP. IP was conducted according to our previous report with some modifications [60]. In brief, after anesthetizing the mice with chloral hydrate (400 mg/kg mouse) dissolved in PBS intraperitoneally, their dorsal skin was shaved for IP application. Then, moistened nonwoven fabric (0.5 cm^2) containing FITC-labeled oligonucleotide (10 μg/50 μl) was attached to the shaved dorsal skin, and another wetted nonwoven fabric (0.5 cm^2) containing PBS (50 μl) was placed 1 cm away. Each piece of the wetted nonwoven fabric was connected to Ag-AgCl electrodes. The Ag-AgCl electrodes with nonwoven fabric containing labeled oligonucleotide or PBS were connected to the cathode and anode, respectively, of a power supply (TTI Ellebeau, Inc., model TCCR-3005, Tokyo, Japan). IP was performed with a fixed current of 0.17 mA/0.5cm^2 for 1 h. Finally, mice were incubated for 3 h, followed by excision of their skin for cross-sectioning.

3.2.4. Intradermal distribution of FITC-labeled oligonucleotide after applying iontophoresis

Mice were euthanized after the incubation time (3 h), and their skin was excised, embedded in OCT compound, and then frozen with dry ice/ethanol. Sections (10 μm thick) were cut from the frozen blocks using a cryostat (CM3050S; Leica Biosystems, Tokyo, Japan). Dako fluorescence mounting medium was used for mounting the 10 μm thick frozen sections onto MAS-coated glass slides. Finally, the skin sections were stored in the dark until dry for subsequent observation of intradermal distribution of the labeled oligonucleotide using CLSM (LSM700, Carl Zeiss, Jena, Germany).

3.2.5. Preparation of minimal naked mRNA vaccine as a potential melanoma therapeutic

Capped 62-nt mRNA encoding decapeptide MKVPRNQDWL, which is shown as 5′_m^7G(5′)ppp(5′)_G_m_G_m_AGCCACCAUGAAGGUGCCCCGGAACCAGGACUGGCUG UGAAAAAAAAAAAAAAAAAAAA_3′ (m^7G, 7-methyl-G; G_m, 2′-*O*-methyl-G), was synthesized according to a previous report [136]. Briefly, 5′ phosphorylated 62-nt RNA was synthesized using standard phosphoramidite chemistry on an automated DNA/RNA synthesizer. RNA was deprotected in a 1:1 mixture of 40% aqueous methylamine and 28% ammonium solution at 65°C for 20 min, followed by overnight treatment with 1 M tetrabutylammonium fluoride (TBAF) in tetrahydrofuran (THF) solution at room temperature. Deprotected RNA was then purified by reversed-phase HPLC (RP-HPLC). The synthesized 5′ phosphorylated RNA was chemically capped using 7-methylguanosine diphosphate imidazolide (Im-m^7GDP) in a reaction mixture of 20 M RNA, 10 mM Im-m^7GDP, 10 mM $CaCl_2$, and 10 mM 2-nitroimidazole in dimethyl sulfoxide (DMSO). First, aqueous solutions of RNA and $CaCl_2$ were mixed and lyophilized. After being suspended in

DMSO, DMSO solutions of Im-m^{7}GDP and 2-nitroimidazole were added. The mixture was heated at 55°C for 3 h, followed by RNA recovery via alcohol precipitation. Capped RNA was further purified by RP-HPLC. After purification, capped RNA was alcohol-precipitated and re-dissolved with water. The RNA concentration was measured based on absorbance at 260 nm using a NanoDrop 2000 spectrophotometer (Thermo). Capped mRNA was analyzed by liquid chromatography-mass spectrometry using an Agilent 1260 Infinity II LC/MSD system, and the mass was found to match the theoretical mass: calcd, 20,732.63; found 20,735.64 (+3.01).

3.2.6. Therapeutic effect of iontophoretic-delivered minimal mRNA vaccine on tumor regression

Male C57BL/6J mice (6 weeks old) were subcutaneously inoculated into their flank with B16F1 cells (10^5 cells/mouse) suspended in PBS (day 0). The mRNA vaccine therapeutic was initiated on day 5 after tumor cells inoculation. Five doses of vaccine were administered every 3 days for a total of 13 days. Mice were immunized by a fixed volume (30 μg/50 μl/dose mouse) of mRNA vaccine, which was administered via one of two routes, namely s.c injection (near the tumor site) or IP (above the tumor site). IP was carried out at 0.17 mA/0.5 cm^2 for 1 h as described above. Tumor burden was determined every other day using a digital caliper according to the following equation: T_{vol} (mm^3) = length × width^2 × 0.5. At day 22 after tumor cells inoculation mice were euthanized and the skin, spleen and tumor tissues were harvested and stored at -80°C for further analysis.

3.2.7. RNA extraction

Skin tissue (90 mg) and tumor tissue (45 mg) were weighed and subsequently homogenized in the presence of 1 ml of ISOGEN Lysis reagent using TissueRuptor II (QIAGEN). The homogenate was then incubated for 5 min at room temperature. Finally, ISOGEN with Spin Column RNA extraction reagent was used for purifying and extracting the total RNA according to the manufacturer's instructions. Total RNA concentration and purity were measured with a Nanodrop 8000 (Thermo Fisher Scientific, DE, USA).

3.2.8. RT-PCR for quantitative analysis of various cytokines in different tissues

cDNA was prepared from the reverse transcription of 2 μg of total RNA extract using PrimeScript^{TM} RT Master Mix and a MJ Mini Personal Thermal Cycler (BioRad Laboratories, Hercules, CA). The reverse transcription reaction was conducted at 37°C for 15 min, while inactivation of reverse transcriptase was conducted at 85°C for 5 min. RT-PCR analysis was performed using TB Green™ Premix Ex Taq™ II and a Thermal Cycler Dice Real Time System III (Takara Bio). For analysis of the mRNA expression levels of IFN-γ, TNF-α, IL-6, IL-12b and GAPDH, cDNA was denatured at 95°C for 30 s, followed by 40 cycles of 95°C for 5 s and 60°C for 30 s for amplification. The mRNA expression levels of IFN-γ, TNF-α, IL-6 and IL-12b were calculated using the $2^{-\Delta\Delta Ct}$ method by normalization relative to GAPDH mRNA.

3.2.9. Investigation of infiltrated cytotoxic $CD8^+$ and $CD4^+$ T cells in the tumor and spleen tissues by immunohistochemistry analysis

At day 22 post tumor cells inoculation in immunized mice, the tumor and spleen tissues were collected, embedded in OCT and stored at -80°C, as described above. Then, frozen blocks of tumor and spleen tissues were cut into 10 μm thick sections using a cryostat (CM3050S; Leica Biosystems, Tokyo, Japan), and subsequently immunostained for both $CD8^+$ and $CD4^+$ T cells.

Tissue sections were washed first by PBS, followed by blocking with 1.5 % BSA dissolved in PBS containing 0.1% Tween-20 for 15 min at room temperature. Tissue sections were then incubated with the diluted rabbit anti-mouse CD8 and CD4 primary antibodies separately for 18 h at 4°C. Then, the sections were incubated with the diluted Alexa 488-labeled goat anti-rabbit IgG for 1 h at room temperature. DAPI was used for staining the nucleus. Finally, tissue sections were mounted with dako fluorescence mounting medium and allowed to dry. The sections were observed using CLSM (LSM700, Carl Zeiss, Jena, Germany).

3.2.10. ELISA

Male C57BL/6J mice (6 weeks old) were subcutaneously inoculated into their flank with B16F1 cells (10^5 cells/mouse) (day 0). Mice were immunized with 5 doses of mRNA vaccine via one of two routes, namely s.c injection or IP as mentioned above. Blood was collected on days 6, 9, 10 and 22 after tumor cells inoculation. Blood samples were stored at 4°C for 3 h followed by centrifugation (Tomy, MX-160, Tokyo, Japan) at 2490 g/30 min for separation of serum, which was stored at -80°C until assayed. Finally, serum IFN-γ levels were determined by sandwich ELISA using Quantikine kit (MIF00, R&D Systems).

3.2.11. Statistical analysis

One-way ANOVA with Tukey post-hoc test was used for evaluating statistical differences among 3 groups. Data are presented as mean ± S.D.

3.3. Results

3.3.1. Iontophoresis of fluorescent-labeled oligonucleotide

In the present study, the negatively charged, high molecular weight (M.W: 19,800) FITC-labeled oligonucleotide (green signal) was used as a model of mRNA to investigate the potential effect of IP technology on mRNA delivery into skin layers. Non-treated healthy skin was used as a control, which showed the absence of any fluorescence signal (**Fig. 3.12.a**). On the other hand, **Fig. 3.12.b** shows the homogenous distribution of the FITC-labeled oligonucleotide into skin layers to a depth of about 100 μm after IP application.

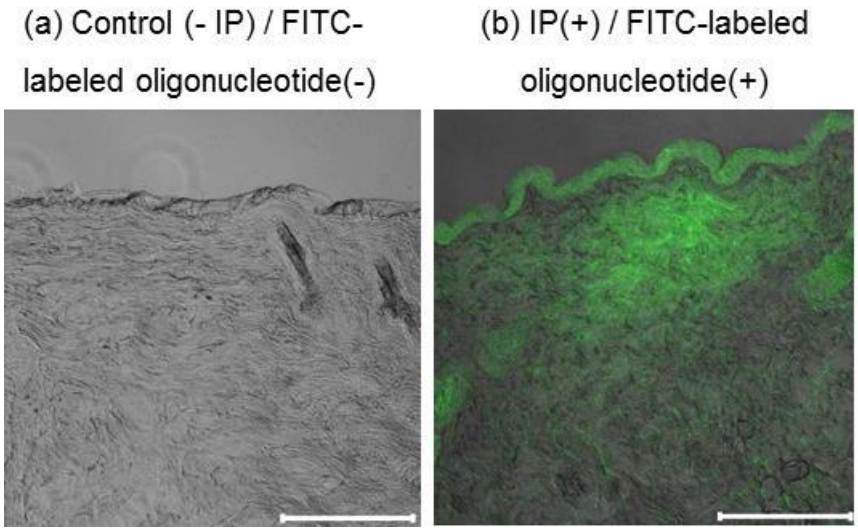

Fig 3.12. Intradermal distribution of FITC-labeled oligonucleotide (green) after IP application.

10 μm thick skin sections were prepared for observation by CLSM. (a) control group (-IP) / FITC-labeled oligonucleotide (-). (b) intradermal distribution of FITC-labeled oligonucleotide after IP application (0.17 mA/0.5 cm^2, 1 h) followed by 3 h incubation. Scale bars = 100 μm.

3.3.2. Effect of iontophoretic-administered therapeutic minimal mRNA vaccine on melanoma inhibition

Mice bearing melanoma were treated with the minimal naked mRNA vaccine by different routes (either s.c. injection or IP). As predicted, a significant regression in tumor volume was observed after IP application compared to non-vaccinated mice, with an exception at days 10 and 12, in which no significant difference was observed (**Fig. 3.13**). On the other hand, s.c injection of the minimal mRNA vaccine did not show a significant reduction in tumor volume at all days except for the last day (day 22), in which a slight significant difference was noted compared to non-vaccinated mice (**Fig. 3.13**). Further, when comparing IP application and s.c injection, there was a significant difference noted at days 16, 20 and 22**.**

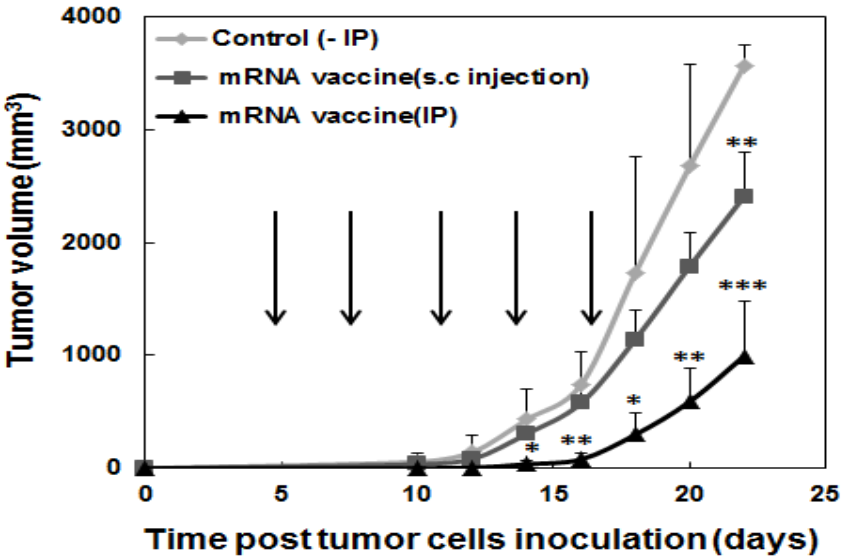

Fig 3.13. Therapeutic effect of minimal mRNA vaccine on tumor inhibition.

After inoculating mice with B16F1 cells (day 0), 5 doses of therapeutic minimal mRNA vaccine were administered every 3 days (indicated by arrows) by different routes, namely s.c. injection (near the tumor site) or IP (above the tumor site). Tumor volume was measured every other day using a digital caliper. Values represent the mean ± SD (n = 4). (*P < 0.05, **P < 0.01, ***P < 0.0001).

3.3.3. The role of cytokines production and infiltration of cytotoxic $CD8^+$ T cells in inhibiting melanoma growth after immunization with iontophoretic-administered minimal mRNA vaccine

Reduction in tumor volume was likely due to the infiltration of cytotoxic tumor-specific $CD8^+$ T cells into the tumor microenvironment, in addition to the secretion of the most critical inflammatory cytokine, IFN-γ, for tumor regression. To confirm these hypotheses, mRNA expression levels of various cytokines, including IFN-γ, TNF-α, IL-6 and IL-12b, were detected by RT-PCR. Results revealed a significant difference in mRNA expression levels of all cytokines in both skin and tumor tissues in the IP-vaccinated group compared to either the non-vaccinated group or the s.c-vaccinated group, with an exception only for IL-6 in the tumor tissue, in which no significant difference was observed (**Figs. 3.14**). Furthermore, the s.c- vaccinated group did not show any significant difference compared to the non-vaccinated group (**Figs. 3.14**).

Based on these findings, I analyzed tumor and spleen tissues for infiltrated cytotoxic $CD8^+$ and $CD4^+$ T cells. **Figures. 3.15** show infiltration of both cytotoxic $CD8^+$ and $CD4^+$ T cells (green signals) in both tumor and spleen tissues in the IP-vaccinated group compared with the non-vaccinated group.

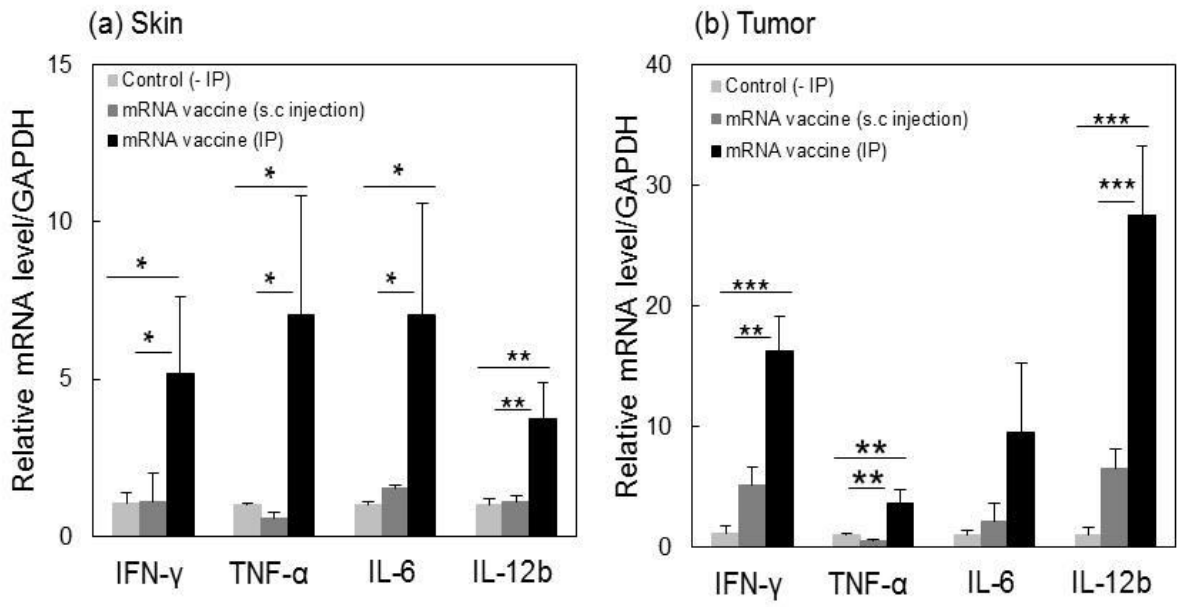

Fig 3.14. Quantitative analysis of mRNA expression levels of inflammatory cytokines in different tissues of mRNA-vaccinated mice.

(a) skin tissue and (b) tumor tissue. Mice were immunized with the minimal mRNA vaccine via IP (above the tumor site) or s.c. injection (near the tumor site) as mentioned previously. At day 22 after tumor cells inoculation, mice were euthanized and tissues were collected. Quantitative evaluation of mRNA expression levels of different cytokines, namely IFN-γ, TNF-α, IL-6 and IL-12b, using RT-PCR was performed. Data are mean ± S.D. ($n = 3$). (*$P < 0.05$, **$P < 0.01$, ***$P < 0.001$).

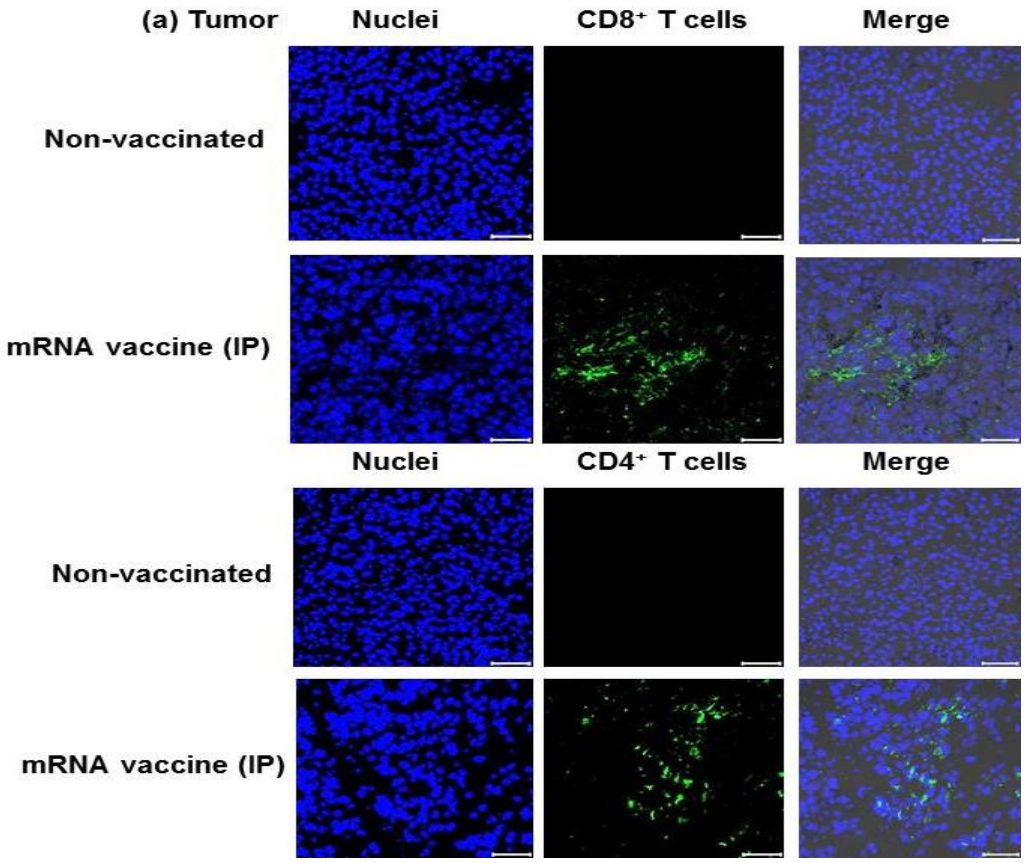

Fig 3.15.a. Immunohistochemical detection of infiltrated cytotoxic $CD8^+$ and $CD4^+$ T cells in tumor tissue.

Tumor tissue was collected at day 22 after tumor cells inoculation in mice immunized with the minimal mRNA vaccine using IP (above the tumor site). (a) tumor tissue. $CD8^+$ and $CD4^+$ T cells are represented by the green (Alexa 488) fluorescence. Nuclei are stained blue (DAPI). Scale bars = 50 μm.

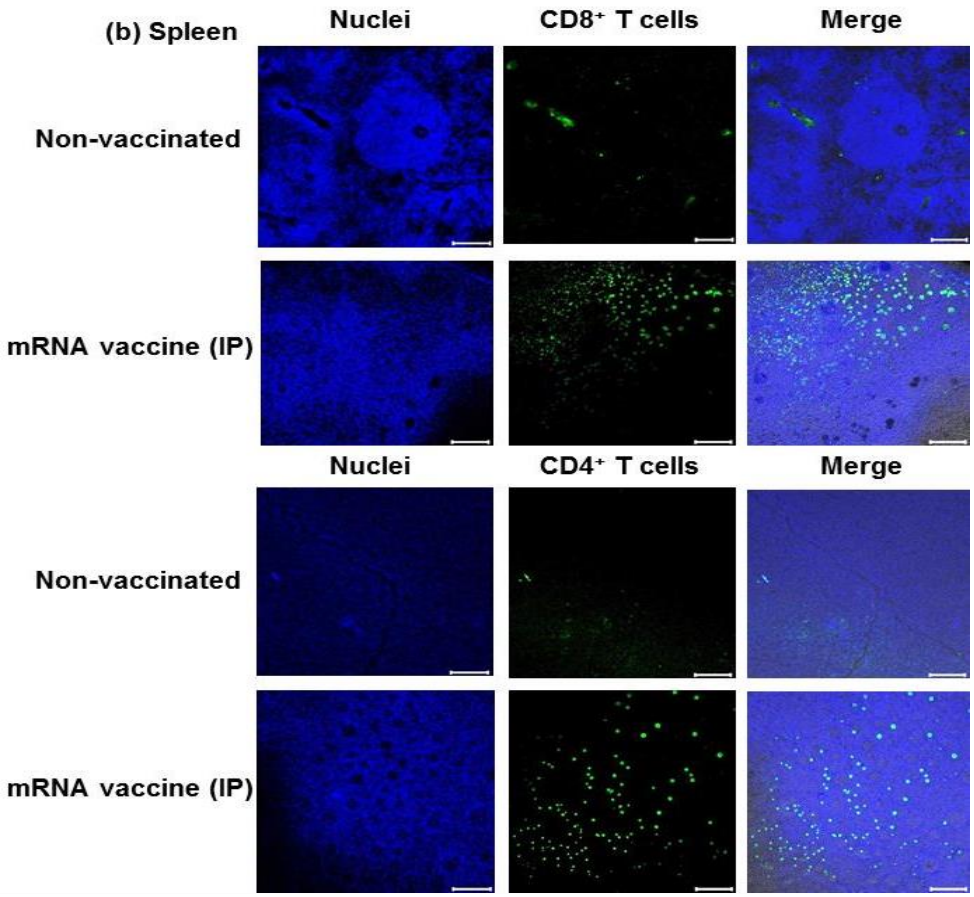

Fig 3.15.b. Immunohistochemical detection of infiltrated cytotoxic $CD8^+$ and $CD4^+$ T cells in spleen tissue.

Spleen tissue was collected at day 22 after tumor cells inoculation in mice immunized with the minimal mRNA vaccine using IP (above the tumor site). (b) spleen tissue. $CD8^+$ and $CD4^+$ T cells are represented by the green (Alexa 488) fluorescence. Nuclei are stained blue (DAPI). Scale bars = 50 μm.

3.3.4. Iontophoretic delivery of therapeutic minimal mRNA vaccine enhanced systemic immunity

Finally, to evaluate the potency of minimal mRNA vaccine in inducing a systemic immune response, serum IFN-γ levels were detected at various days following vaccination. Serum IFN-γ levels were significantly different in the s.c- and IP- vaccinated groups compared with the non-vaccinated group, with an exception at day 9 for the s.c-injected group. However, there was a non-significant difference between the s.c- and IP- vaccinated groups at days 6, 9, and 10, while serum IFN-γ levels in the IP-vaccinated group were slightly higher than those in the s.c-vaccinated group. Moreover, at day 22 following the full 5-doses treatment, IFN-γ serum level in the IP-vaccinated group was significantly upregulated (11.83±0.87 pg/mL) compared to the s.c-vaccinated group (1.49±0.18 pg/mL) (**Fig.3.16**).

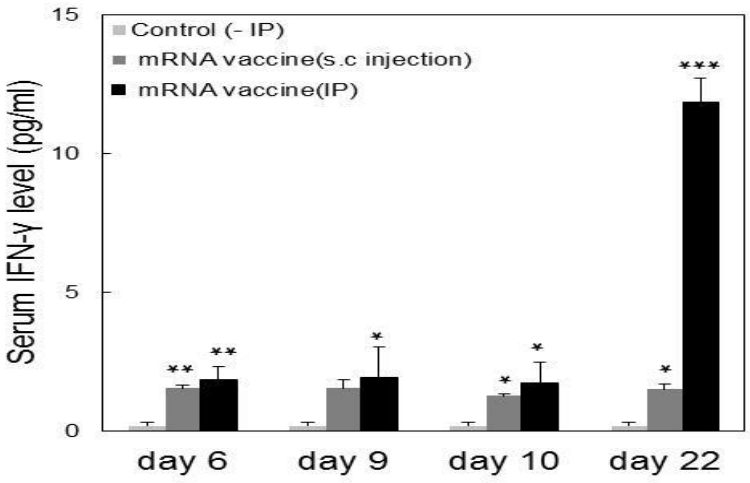

Fig 3.16. Detection of serum IFN-γ levels at different time intervals in mice bearing melanoma treated with the minimal mRNA vaccine.

After inoculating mice with B16F1 cells (day 0), mice were treated with the minimal mRNA vaccine via IP (above the tumor site) or s.c injection (near the tumor site). At days 6, 9, 10 and 22 post tumor cells inoculation, blood was withdrawn for determination of IFN-γ serum levels. Data are mean ± S.D. (n = 3). (*P < 0.05, **P < 0.01, ***P < 0.0001).

3.4. Discussion

IP application was successful at inducing a homogenous distribution of the high molecular weight FITC-labeled oligonucleotide in the epidermal layer of the skin (**Fig.3.12.b**). Penetration of the FITC-labeled oligonucleotide to depths of 100 μm after IP application indicates its accumulation within the epidermal layer, which ranges from 100 to 200 μm in thickness [70]. Consequently, the FITC-labeled oligonucleotide can be engulfed by the epidermal LCs for subsequent activation of an immune response. I subsequently investigated therapeutic outcomes following immunization of mice bearing melanoma with a non-formulated naked minimal mRNA vaccine encoding TAA human gp100 $_{(25\text{-}33)}$ (KVPRNQDWL) using IP. It has been reported that inclusion of a short poly (A) tail can simplify mRNA preparation, as well as improve its stability and enhance intracellular translation [136]. Therefore, a minimal mRNA vaccine with a short poly (A) tail 20-nt (M.W: 20,460) was chemically synthesized. Furthermore, mRNA is known to be highly negatively charged, which impairs its intracellular uptake [123,125,129,130]. Consequently, in this study I anticipated that IP application would not only improve the delivery of minimal mRNA into skin layers, but also enhance intracellular uptake by APCs as reported previously for IP delivery of siRNA [137,138]. In a more detail, the effect of various endocytosis inhibitors (e.g., amiloride, filipin, sucrose, and low temperature exposure) was studied and after visualization by confocal microscopy, the IP-induced cellular uptake pathway of siRNA (M.W: 1**2,**000) was found to be due to the activation of many specific signaling molecules related to endocytosis [137]. Additionally, endosomes were found to leak macromolecules exhibiting molecular weights <70,000 [138]. Thereby, a minimal mRNA with a lower molecular weight (M.W: 20,460) that can achieve an endosomal escape was prepared. A potent immune response was therefore expected by combining the minimal mRNA therapeutic with IP technology. The tumor regression after immunization (**Fig.3.13**)

demonstrates the successful delivery of a minimal mRNA vaccine using IP technology, resulting in subsequent stimulation of an immune response.

Following IP application, the minimal mRNA vaccine was likely distributed homogenously into skin layers, where epidermal immune cells reside, mainly LCs that can extend their dendrites and survey the skin to capture the vaccine, resulting in subsequent cytoplasmic delivery of the vaccine via cellular uptake [68,96,110]. Reduction in tumor volume was likely due to infiltration of cytotoxic tumor-specific $CD8^+$ T cells into the tumor microenvironment, in addition to secretion of the most critical inflammatory cytokine, IFN-γ, for tumor regression [69,72,78,111,116]. The cytokines likely contributed to fighting melanoma growth via various mechanisms, including activation of adaptive immunity [96,109,117,118]. IL-12b plays a role in upregulating the secretion of IFN-γ, which is considered one of the key factors for tumor regression based on its ability to: inhibit angiogenesis, increase intra-tumoral levels of MHC I and II molecules, and promote apoptosis [69,111,116,119,120,141]. Moreover, IFN-γ augments the differentiation of cytotoxic $CD8^+$ T cells, which are known to have a lethal effect on tumor cells [68]. Consequently, both IFN-γ and IL-12b are considered crucial cytokines for activating adaptive immunity. Moreover, other proinflammatory cytokines, particularly TNF-α and IL-6, also play a critical role in eliciting an immune response by enhancing the trafficking of DCs toward the DLNs and the infiltration of cytotoxic $CD8^+$ T cells in the tumor tissue [68,69,116,121,142]. Infiltration of cytotoxic $CD8^+$ and $CD4^+$ T cells in the tumor microenvironment is critical for tumor regression, as previously noted and these results demonstrate the ability of IP-administered minimal mRNA vaccine to elicit cell-mediated adaptive immunity, which is considered a main element required for tumor clearance [143-146].

Finally, serum IFN-γ levels demonstrate the ability of the minimal mRNA vaccine to induce and maintain a systemic immune response via permanent stimulation of skin resident immune cells [96]. Moreover, delivery of the minimal mRNA vaccine via IP showed a significant melanoma regression, elevation in cytokine expression levels, and induction of systemic immunity at day 22 compared to s.c injection. These findings are likely driven by the unique features of IP technology in being able to homogeneously distribute and accumulate the minimal mRNA vaccine into skin layers, and subsequently expose it for engulfment by skin-abundant immune cells in addition to improving intracellular uptake of the vaccine. On the other hand, the minimal mRNA vaccine is expected to quickly diffuse after s.c injection, which can impair the activation of APCs. Results of this study demonstrate successful immune system activation and melanoma regression by combining a newly synthesized minimal mRNA vaccine with IP technology, and offer a new step in the field of mRNA vaccination.

3.5. Conclusion

In conclusion, I demonstrated the efficiency of IP technology in overcoming challenges associated with the stratum corneum for the delivery of a non-formulated minimal mRNA vaccine encoding TAA against melanoma growth. As expected, a potent immune response was induced after combining IP technology with the minimal mRNA vaccine, which resulted in tumor inhibition and upregulation of cytokine expression levels, as well as infiltration of cytotoxic $CD8^+$ and $CD4^+$ T cells into the tumor microenvironment. To my knowledge, this is the first report demonstrating the successful combination of IP and chemically synthesized minimal mRNA vaccine.

Chapter IV

Conclusion and Future Perspectives

Chapter IV: Conclusion and Future Perspectives

Conclusion

The outcomes of this thesis could be summarized as follows:

Chapter II

- IP technology showed a success in distributing the prophylactic polyplex vaccine homogenously into the skin.
- IP-administered polyplex vaccine elicited an immune response which exhibited either a prophylactic or therapeutic effect against melanoma growth.

Chapter III

- IP technology showed a success in delivering the minimal mRNA vaccine, which was obvious through tumor inhibition in mice bearing melanoma.
- Combining IP technology with the minimal mRNA vaccine showed a significant and potent effect compared with s.c injection, which showed a weak effect.

Future perspectives

Despite IP's success in delivering hydrophilic macromolecules into the skin, researchers must pay more attention toward whether it is possible to apply IP technology to young ages or not. Additionally, the development of other safe prophylactic vaccines for non-viral cancers must be taken into consideration. Finally, although the naked non-formulated minimal mRNA vaccine showed significant effects, complete protection against skin nucleases is required for getting more potent effect.

Acknowledgments & Dedication

I am deeply thankful to the God, **ALLAH,** who helped me to reach my goal and gave me the power to finish this work.

I would like to express my gratitude and profound indebtedness to my **Prof.Dr.Kentaro Kogure,** Professor of pharmaceutical Health chemistry, Graduate School of Pharmaceutical Science, The University of Tokushima; for advice, sincere suggestion, indispensable help, and for providing the facilities during the work of this study.

I wish to express my thankfulness, appreciation and profound gratitude to **Prof.Dr.Hiroshi Abe,** Professor of chemistry, Graduate School of Science, The University of Nagoya, for providing the facilities for completing the work of this study.

I would like to express my heartfelt gratitude to **my colleagues Mr.Daichi Tanaka, Mr. Shinya Inoue, Mr.Shintaro Yoneda and to the spirit of Mr.Dai Majima**; for their technical assistance, and encouragement. Their support has been instrumental in the completion of this study.

I would like to thank all members of pharmaceutical Health chemistry, Graduate School of Pharmaceutical Science, The University of Tokushima, for their kind help.

Finally, my deep thanks to my family for their love, encouragement and patience that pushed me to continue this work and not to give up.

I want to dedicate this thesis to my lovely mother, my sister, my brothers and the spirit of my lovely father.

Rabab, 2023

References

References

[1] Fitzmaurice C, Abate D, Abbasi N, Abbastabar H, Abd-Allah F, Abdel- Rahman O, Abdelalim A Abdoli A, Abdollahpour I. Global, Regional, and National Cancer Incidence, Mortality, Years of Life Lost, Years Lived With Disability, and Disability-Adjusted Life-Years for 29 Cancer Groups, 1990 to 2017: A Systematic Analysis for the Global Burden of Disease Study. JAMA. Oncol., 5, 1749-1768 (2019).

[2] Akkın S, Varan G, Bilensoy E. A Review on Cancer Immunotherapy and Applications of Nanotechnology to Chemoimmunotherapy of Different Cancers. Molecules., 26, 1-24 (2021).

[3] Waldman AD, Fritz JM, Lenardo MJ. A guide to cancer immunotherapy: From T cell basic science to clinical practice. Nat. Rev. Immunol., 20, 651-668 (2020).

[4] Oldham RK. Cancer Biotherapy: More than Immunotherapy. Cancer Biother. Radiopharm., 32, 111-114 (2017).

[5] Yang Y. Cancer immunotherapy: Harnessing the immune system to battle cancer. J. Clin. Investig., 125, 3335-3337 (2015).

[6] Yang M, Olaoba OT, Zhang C, Kimchi ET, Staveley-O'Carroll KF, Li G. Cancer Immunotherapy and Delivery System: An Update. Pharmaceutics., 14, 1-27 (2022).

[7] Ventola CL. Cancer Immunotherapy, Part 3: Challenges and Future Trends. Pharm. Ther., 42, 514-521 (2017).

[8] Zaretsky JM, Garcia-Diaz A, Shin DS, Escuin-Ordinas H, Hugo W, Hu-Lieskovan S, Torrejon DY, Abril-Rodriguez G, Sandoval S, Barthly L. Mutations Associated with Acquired Resistance to PD-1 Blockade in Melanoma. N. Engl. J. Med., 375, 819-829 (2016).

[9] Riley RS, June CH, Langer R, Mitchell MJ. Delivery technologies for cancer immunotherapy. Nat. Rev. Drug Discov., 18, 175-196 (2019).

[10] Ventola CL. Cancer Immunotherapy, Part 1: Current Strategies and Agents. Pharm. Ther., 42, 375-383 (2017).

[11] Zhao Z, Zheng L, Chen W, Weng W, Song J, Ji J. Delivery strategies of cancer immunotherapy: recent advances and future perspectives. J. Hematol. Oncol., 12, 1-14 (2019).

[12] FDA. Center for Biologics Evaluation and Research (CBER). What Are "biologics" Questions and Answers. 2018.

[13] Guo Q, Jiang C. Delivery strategies for macromolecular drugs in cancer therapy. Acta. Pharm. Sin. B., 10, 979-986 (2020).

[14] Mullad A. 2020 FDA drug approvals. Nat. Rev. Drug Discov., 20, 85-90 (2021).

[15] Anselmo A, Gokarn Y, Mitragotri S. Non-invasive delivery strategies for biologics. Nat. Rev. Drug Discov., 18, 19-40 (2018).

[16] Hasan M, Khatun A, Kogure K. Iontophoresis of Biological Macromolecular Drugs. Pharmaceutics., 14, 1-16 (2022).

[17] Chung SW, Hil-Lal TA, Byun Y. Strategies for non-invasive delivery of biologics. J. Drug Target., 20, 481-501 (2012).

[18] Miller MA, Pisani E. The cost of unsafe injections. Bull. World Health Organ., 77, 808-811 (1999).

[19] Gill HS, Prausnitz MR. Does needle size matter?. J. Diabetes Sci. Technol., 1, 725-729 (2007).

[20] Norman JJ, Prausnitz MR. Improving patient acceptance of insulin therapy by improving needle design. J. Diabetes Sci. Technol., 6, 336-338 (2012).

[21] Rohrer J, Lupo N, Bernkop-Schnürch A. Advanced formulations for intranasal delivery of biologics. Int. J. Pharm., 553, 8-20 (2018).

[22] Montenegro-Nicolini M, Morales JO. Overview and future potential of buccal mucoadhesive films as drug delivery systems for biologics. AAPS PharmSciTech., 18, 3-14 (2016).

[23] Senel S, Mremer M, Nagy K, Squire C. Delivery of bioactive peptides and proteins across oral (buccal) mucosa. Curr. Pharm. Biotechnol., 2, 175-186 (2001).

[24] Menon GK, Cleary GW, Lane ME. The structure and function of the stratum corneum. Int. J.Pharm., 435, 3-9 (2012).

[25] Alkilani AZ, McCrudden MTC, Donnelly RF. Transdermal drug delivery: Innovative pharmaceutical developments based on disruption of the barrier properties of the stratum corneum. Pharmaceutics., 7, 438-470 (2015).

[26] Prausnitz MR, Langer R. Transdermal drug delivery. Nat. Biotechnol., 26, 1261-1268 (2008).

[27] Homayun B, Lin X, Choi HJ. Challenges and recent progress in oral drug delivery systems for biopharmaceuticals. Pharmaceutics., 11, 1-29 (2019).

[28] Wysocki AB. Skin anatomy, physiology, and pathophysiology. Nurs. Clin. N. Am., 34, 777-797 (1999).

[29] Palmer BC, DeLouise LA. Nanoparticle-Enabled Transdermal Drug Delivery Systems for Enhanced Dose Control and Tissue Targeting. Molecules., 21, 1-17 (2016).

[30] Matsui T, Amagai M. Dissecting the formation, structure, and barrier function of stratum corneum. Int. Immunol., 27, 269-280 (2015).

[31] Morales JO, Fathe KR, Brunaugh A, Rerrati S, Li S, Montenegro-Nicolini M, Mousavikhamene Z, McConville JT, Prausnitz MR, Smyth HDC. Challenges and future prospects for the delivery of biologics: Oral mucosal, pulmonary, and transdermal routes. AAPS J., 19, 652-668 (2017).

[32] Toll R, Jacobi U, Richter H, Laddermann J, Schaefer H, Blume-Peytavi U. Penetration profile of microspheres in follic-ular targeting of terminal hair follicles. J. Investig. Dermatol., 123, 168-176 (2004).

[33] Peña-Juárez MC, Guadarrama-Escobar OR, Escobar-Chávez JJ. Transdermal Delivery Systems for Biomolecules. J. Pharm. Innov., 17, 1-14 (2021).

[34] Karande P, Mitragotri S. Enhancement of transdermal drug delivery via synergistic action of chemicals. Biochim. Biophys. Acta., 1788, 2362-2373 (2009).

[35] Ashtikar M, Nagarsekar K, Fahr A. Transdermal delivery from liposomes formulations: Evaluation of technology over the last three decades. J. Control. Release., 242, 126-140 (2016).

[36] Venuganti VVK, Perumal OP. Effect of poly (amidoamine) (PAMAM) dendrimer on skin permeation of 5-fluorouracil. Int. J. Pharm., 361, 230-238 (2008).

[37] Wang Y, Su W, Li Q, Li C, Wang H, Li Y, Cao Y, Chang J, Zhang L. Preparation and evaluation of lidocaine hydrochloride-loaded TAT-conjugated polymeric liposomes for transdermal delivery. Int. J. Pharm., 441, 748-756 (2013).

[38] Kováčik A, Kopecˇná M, Vávrová K. Permeation enhancers in transdermal drug delivery: Benefits and limitations. Expert Opin. Drug Deliv., 17, 145-155 (2020).

[39] Lasch J, Laub R, Wohlrab W. How deep do intact liposomes penetrate into human skin?. J. Control. Release., 18, 55-58 (1992).

[40] Ita K. Transdermal iontophoretic drug delivery: Advances and challenges. J. DrugTarget., 24, 386-391 (2015).

[41] Ita K. Perspectives on Transdermal Electroporation. Pharmaceutics., 8, 1-14 (2016).

[42] Polat BE, Hart D, Langer R, Blankschtein D. Ultrasound-mediated transdermal drug delivery: Mechanisms, scope, and emerging trends. J. Control. Release., 152, 330-348 (2011).

[43] Daradhar S, Majumdar A, Dhoble S, Patravale V. Microneedles for transdermal drug delivery: A systemic review. Drug Dev. Ind. Pharm., 45, 188-201 (2018).

[44] Simmons JA, Davis J, Thomas J, Lopez J, Le Blanc A, Allison H, Slook H, Lewis P, Holtz J, Fisher P. Characterization of skin blebs from intradermal jet injection: Ex-vivo studies. J. Control. Release., 307, 200-210 (2019).

[45] Szunerists S, Boukherroub R. Heat: A highly efficient skin enhancer for transdermal drug delivery. Front. Bioeng. Biotechnol., 6, 1-13 (2018).

[46] Kalia YN, Naik A, Garrison J, Guy R. Iontophoretic drug delivery. Adv. Drug Deliv. Rev., 56, 619-658 (2004).

[47] Hasan M, Khatun A, Fukuta T, Kogure K. Noninvasive transdermal delivery of liposomes by weak electric current. Adv. Drug Deliv. Rev., 154-155, 227-235 (2020).

[48] Subramony JA, Sharma A, Phipps J. Microprocessor controlled transdermal drug delivery. Int. J. Pharm., 317, 1-6 (2006).

[49] Gratieri T, Alberti I, Lapteva M, Kalia YN. Next generation intra- and transdermal therapeutic systems: Using non- and minimally-invasive technologies to increase drug delivery into and across the skin. Eur. J. Pharm. Sci., 50, 609-622 (2013).

[50] Roustit M, Blaise S, Cracowski JL. Trials and tribulations of skin iontophoresis in therapeutics. Br. J. Clin. Pharmacol., 77, 63-71 (2015).

[51] Sieg A, Guy R, Delgado-Charro MB. Electroosmosis in transdermal iontophoresis: Implications for noninvasive and calibration- free glucose monitoring. Biophys. J., 87, 3344-3350 (2004).

[52] Pikal MJ. The role of electroosmotic flow in transdermal iontophoresis. Adv. Drug Deliv. Rev., 46, 281–305 (2001).

[53] Curdy C, Kalia YN, Guy RH. Post-iontophoresis recovery of human skin impedance *in vivo*. Eur. J. Pharm. Biopharm., 53, 15-21 (2002).

[54] Hama S, Kimura Y, Mikami A, Shiota K, Toyoda M, Tamura A, Nagasaki Y, Kanamura K, Kajimoto K, Kogure K. Electric stimulus opens intracellular space in skin. J. Biol. Chem., 289, 2450-2456 (2014).

[55] Kigasawa K, Kajimoto K, Hama S, Saito A, Kanamura K, Kogure K. Noninvasive delivery of siRNA into the epidermis by iontophoresis using an atopic dermatitis-like model rat. Int. J. Pharm., 383, 157-160 (2010).

[56] Fukuta T, Oshima Y, Michiue K, Tanaka D, Kogure K. Non-invasive delivery of biological macromolecular drugs into the skin by iontophoresis and its application to psoriasis treatment. J. Control. Release., 323, 323-332 (2020).

[57] Bode C, Zhao G, Steinhagen F, Kinjo T, Klinman DM. CpG DNA as a vaccine adjuvant. Expert Rev. Vaccines., 10, 499-511 (2011).

[58] Knuefermann P, Baumgarten G, Koch A, Schwederski M, Velten M, Ehrentraut H, Mersmann J, Meyer R, Hoeft A, Zacharowski K. CpG oligonucleotide activates Toll-like receptor 9 and causes lung inflammation *in vivo*. Respir. Res., 8, 1-9(2007).

[59] Kigasawa K, Kajimoto K, Nakamura T, Hama S, Kanamura K, Harashima H, Kogure K. Noninvasive and efficient transdermal delivery of CPG-oligodeoxynucleotide for cancer immune therapy. J. Control. Release., 150, 256-265 (2011).

[60] Hasan M, Fukuta T, Inoue S, Mori H, Kagawa M, Kogure K. Iontophoresis-mediated direct delivery of nucleic acid therapeutics, without use of carriers, to internal organs via non-blood circulatory pathways. J. Control. Release., 343, 392-399 (2022).

[61] Wang Y, Zeng L, Song W, Liu J. Influencing factors and drug application of iontophoresis in transdermal drug delivery: An overview of recent progress. Drug Deliv. Transl. Res., 12, 15-26 (2021).

[62] Zhu L, Yang Q, Hu R, Li Y, Peng Y, Liu H, Ye M, Zhang B, Zhang P, Liu-Smith F, Li H, Liu J. Novel therapeutic strategy for melanoma based on albendazole and the CDK4/6 inhibitor palbociclib. Nature. Portfolio., 12, 1-10 (2022).

[63] Conte S, Ghazawi FM, Le M, Nedjar H, Alake A, Lagacé F, Mukovozov IM, Cyr J, Mourad A, Miller WH, Claveau J, Salopek TG, Netchiporouk E, Gniadecki R, Sasseville D, Rahme E, Litvinov IV. Population-Based Study Detailing Cutaneous Melanoma Incidence and Mortality Trends in Canada. Front. Med., 9, 1-11 (2022).

[64] Saginala K, Barsouk A, Aluru JS, Rawla P, Barsouk A. Epidemiology of Melanoma. Med. Sci., 9, 1-9 (2021).

[65] Berk-Krauss J, Stein JA, Weber J, Polsky D, Geller AC. New Systematic Therapies and Trends in Cutaneous Melanoma Deaths Among US Whites, 1986–2016. AJPH., 110, 731-733 (2020).

[66] Labala S, Jose A, Chawla SR, Khan MS, Bhatnagar S, Kulkarni OP, Venuganti VVK. Effective melanoma cancer suppression by iontophoretic co-delivery of STAT3 siRNA and imatinib using gold nanoparticles. Int. J. Pharm., 525, 407-417 (2017).

[67] Carè A, Bufalo DD, Facchiano A. Editorial on Special Issue "Advances and Novel Treatment Options in Metastatic Melanoma". Cancers., 14, 1-4 (2022).

[68] Cheng R, Fontana F, Xiao J, Liu Z, Figueiredo P, Shahbazi MA, Wang S, Jin J, Torrieri G, Hirvonen JT, Zhang H, Chen T, Cui W, Lu Y, Santos HA. Recombination Monophosphoryl Lipid A-Derived Vacosome for the Development of Preventive Cancer Vaccines ACS. Appl. Mater. Interfaces., 12, 44554-44562 (2020).

[69] Liu J, Fu M, Wang M, Wan D, Wei Y, Wei X. Cancer vaccines as promising immuno-therapeutics: platforms and current progress. J. Hematol. Oncol., 15, 1-26 (2022).

[70] Toyodaa M, Hamaa S, Ikedab Y, Nagasakib Y, Kogure K. Anti-cancer vaccination by transdermal delivery of antigen peptide-loaded nanogels via iontophoresis. Int. J. Pharm., 483 110-114 (2015).

[71] Apostolopoulos V. Cancer Vaccines: Research and Applications. Cancers., 11, 1-5 (2019).

[72] Jaini R, Kesaraju P, Johnson JM, Altuntas CZ, Jane-wit D, Tuohy VK. An autoimmune-mediated strategy for prophylactic breast cancer vaccination. Nat. Med., 16, 799-804 (2010).

[73] Rosenberg SA, Yang JC, Restifo NP. Cancer immunotherapy: moving beyond current vaccines. Nat. Med., 10, 909-915 (2004).

[74] Saxena M, Burg SHV, Melief CJM, Bhardwaj N. Therapeutic cancer vaccines. Nat. Rev. Cancer., 21, 360-378 (2021).

[75] Fusciello M, Fontana F, Tähtinen S, Capasso C, Feola S, Martins B, Chiaro J, Peltonen K, Ylösmäki L, Ylösmäki E, Hamdan F, Kari OK, Ndika J, Alenius H, Urtti A, Hirvonen JT, Santos HA, Cerullo V. Artificially cloaked viral nanovaccine for cancer immunotherapy. Nat. Commun. 10, 1-13 (2019).

[76] Wang T, Wang D, Yu H, Feng B, Zhou F, Zhang H, Zhou L, Jiao S, Li Y. A cancer vaccine-mediated postoperative immunotherapy for recurrent and metastatic tumors. Nat. Commun., 9, 1-12 (2018).

[77] Farhood B, Najafi M, Mortezae K. $CD8^+$ cytotoxic T lymphocytes in cancer immunotherapy: A review. J. Cell. Physiol., 234, 1-13 (2018).

[78] Scott BA, Yarchoan M, Jaffee EM. Prophylactic Vaccines for Nonviral Cancers. Annu. Rev. Cancer. Biol., 2, 195-211 (2018).

[79] Zhao B, Wang Y, Wu B, Liu S, Wu E, Fan H, Gui M, Chen L, Li C, Ju Y, Zhang W, Meng S. Placenta-derived gp96 as a multivalent prophylactic cancer vaccine. Sci. Rep., 3, 1-7 (2013).

[80] Finn OJ. The dawn of vaccines for cancer prevention. Nat. Rev. Immunol., 18, 183-194 (2018).

[81] Crews DW, Dombroski JA, King MR. Prophylactic Cancer Vaccines Engineered to Elicit Specific Adaptive Immune Response. Front. Oncol., 11, 1-14 (2021).

[82] Frazer IH, Lowy DR, Schiller JT. Prevention of cancer through immunization: Prospects and challenges for the 21st century. Eur. J. Immunol., 37, 148-155 (2007).

[83] Parkin DM. The global health burden of infection-associated cancers in the year 2002. Int. J. Cancer., 118, 3030-3044 (2006).

[84] McCaskill-Stevens W, Pearson DC, Kramer BS, Ford LG, Lippman SM. Identifying and Creating the Next Generation of Community- Based Cancer Prevention Studies: Summary of a National Cancer Institute Think Tank. Cancer Prev. Res., 10, 99-107 (2017).

[85] Pere H, Montier Y, Bayry J, Quintin-Colonna F, et al. A CCR4 antagonist combined with vaccines induces antigen-specific $CD8^+$ T cells and tumor immunity against self-antigens. Blood., 118, 4853-4862 (2011).

[86] Yarchoan M, Johnson BA , Lutz ER, Laheru DA, Jaffee EM. Targeting neoantigens to augment antitumour immunity. Nat. Re. Cancer., 17, 209-222 (2017).

[87] Blass E, Ott PA. Advances in the development of personalized neoantigen- based therapeutic cancer vaccines. Nat. Rev. Clin. Oncol., 18, 215-229 (2021).

[88] Peng M, Mo Y, Wang Y, Wu P, Zhang Y, Xiong F, Guo C, Wu X, Li Y, Li X, Li G, Xiong W, Zeng Z. Neoantigen vaccine: an emerging tumor immunotherapy. Mol. Cancer., 18, 1-14 (2019).

[89] Hollingsworth RE, Jansen K. Turning the corner on therapeutic cancer vaccines. npj Vaccines., 7, 1-10 (2019).

[90] Overwijk WW, Tsung A, Irvine KR, Parkhurst MR, Goletz TJ, Tsung K, Carroll MW, Liu C, Moss B, Rosenberg SA, Restifo NP. gp100/pmel 17 Is a Murine Tumor Rejection Antigen: Induction of "Self"-reactive, Tumoricidal T Cells Using High-affinity, Altered Peptide Ligand. Exp. Med., 188, 277-286 (1998).

[91] Stipdonk MJBV, Badia-Martinez D, Sluijter M, Offringa RI, Hall TV, Achour A. Design of Agonistic Altered Peptides for the Robust Induction of CTL Directed towards H-$2D^b$ in Complex with the Melanoma-Associated Epitope gp100. Cancer Res., 69, 7784-7792 (2009).

[92] Hickman HD, Yewdell JW. Going Pro to enhance T cell immunogenicity: easy as π?. Eur. J. Immunol., 43, 2814-2817 (2013).

[93] Pedersen SR, Sørensen MR, Buus S, Christensen JP, Thomsen AR. Comparison of Vaccine-Induced Effector CD8 T Cell Responses Directed against Self-and Non-Self-Tumor Antigens: Implications for Cancer Immunotherapy. J. Immunol., 191, 3955-3967 (2013).

[94] Aranda F, Vacchelli E, Eggermont A, Galon J, Sautès-Fridman C, Tartour E, Zitvoge L, Kroemer G, GalluzziL. Trial Watch: Peptide vaccines in cancer. OncoImmunology., 2, 1-11 (2013).

[95] Banday AH, Jeelani S, Hruby VJ. Cancer vaccine adjuvants – recent clinical progress and future perspectives. Immunopharmacol. Immunotoxicol., 37, 1-11 (2014).

[96] Kigasawa K, Kajimoto K, Nakamura T, Hama S, Kanamura K, Harashima H, Kogure K. Noninvasive and efficient transdermal delivery of CpG-oligodeoxynucleotide for cancer immunotherapy. J. Control. Release., 30, 256-265 (2011).

[97] Kawasaki T, Kawai T. Toll-like receptor signaling pathways. Front. Immunol., 5, 1-8 (2014).

[98] Chuang Y, Tseng J, Huang L, Huang C, Huang CF, Chuang T. Adjuvant Effect of Toll-Like Receptor 9 Activation on Cancer Immunotherapy Using Checkpoint Blockade Front. Immunol., 11, 1-14 (2020).

[99] Hettinga J, Carlisle R. Vaccination into the Dermal Compartment: Techniques, Challenges, and Prospects. Vaccines., 8, 2-40 (2020).

[100] Wilson DR, Suprenant MP, Miche JH, Wang EB, Tzeng SY, Green JJ. The Role of Assembly Parameters on Polyplex Poly (Beta-Amino Ester) Nanoparticle Transfections. Biotechnol. Bioeng., 116, 1220-1230 (2019).

[101] Dinari A, Moghadam TT, Abdollahi M, Sadeghizadeh M. Synthesis and Characterization of a Nano-Polyplex system of GNRs- PDMAEA-pDNA: An Inert Self-Catalyzed Degradable Carrier for Facile Gene Delivery. Sci. Rep., 8, (2018) 1-12 (2018).

[102] Valente JFA, Pereira P, Sousa A, Queiroz JA, Sousa F. Effect of Plasmid DNA Size on Chitosan or Polyethyleneimine Polyplexes Formulation. Polymers., 13, 1-15 (2021).

[103] Thomas TJ, Tajmir-Riahi H, Pillai CKS. Biodegradable Polymers for Gene Delivery. Molecules., 24, 2-24 (2019).

[104] Meng W, Yamazaki T, Nishida Y, Hanagata N. Nuclease-resistant immunostimulatory phosphodiester CpG oligodeoxynucleotides as human Toll-like receptor 9 agonists BMC. Biotechnol., 11, 1-9 (2011).

[105] Kubo A, Nagao K, Yokouchi M, Sasaki H, Amagai M. External antigen uptake by Langerhans cells with reorganization of epidermal tight junction barriers. J. Exp. Med., 206, 2937-2946 (2009).

[106] Hama S, KimuraY, Mikami A, Shiota K, Toyoda M, Tamura A, Nagasaki Y, Kanamura K, Kajimoto K, Kogure K. Electric Stimulus Opens Intercellular Spaces in Skin. J. Biol. Chem., 289, 2450-2456 (2014).

[107] Sugita K, Kabashima K, Atarashi K, Shimauchi T, Kobayashi M, Tokura Y. Innate immunity mediated by epidermal keratinocytes promotes acquired immunity involving Langerhans cells and T cells in the skin. Clin. Exp. Immunol., 147, 176-183 (2006).

[108] Celluzzi CM, Falo LD. Epidermal Dendritic Cells Induce Potent Antigen-Specific CTL-Mediated Immunity. J. Invest. Dermatol., 108, 716-720 (1997).

[109] Ezepchuk YV, Leung DYM, Middleton MH, Bina P, Reiser R, Norris DA. Staphylococcal Toxins and Protein A Differentially Induce Cytotoxicity and Release of Tumor Necrosis Factor-α From Human Keratinocytes. J. Invest. Dermatol., 107, 603-609 (1996).

[110] Belyakov IM, Hammond SA, Ahlers JD, Glenn GM, Berzofsky JA. Transcutaneous immunization induces mucosal CTLs and protective immunity by migration of primed skin dendritic cells. J. Clin. Investig., 113, 998-1007 (2004).

[111] Nanni P, Nicoletti G, Palladini A, Croci S, Murgo A, Antognoli A, Landuzzi L, Fabbi M, Ferrini S, Musiani P, Iezzi M, De Giovanni C, Lollini P. Antimetastatic Activity of a Preventive Cancer Vaccine. Cancer Res., 67, 11037-12034 (2007).

[112] Sakaguchi S. Naturally arising Foxp3-expressing $CD25^+$ $CD4^+$ regulatory T cells in immunological tolerance to self and non-self. Nat. Immunol., 6, 345-352 (2005).

[113] Cheung AS, Koshy ST, Stafford AG, Bastings MMC, Mooney GJ. Adjuvant-Loaded Subcellular Vesicles Derived From Disrupted Cancer Cells for Cancer Vaccination. Small., 12, 2321-2333 (2016).

[114] Häcker H, Mischak H, Miethke T, Liptay S, Schmid R, Sparwasser T, Heeg K, Lipford GB, Wagner H. CpG-DNA-specific activation of antigen-presenting cells requires stress kinase activity and is preceded by non-specific endocytosis and endosomal maturation. EMBO. J., 17, 6230-6240 (1998).

[115] Kawarada Y, Ganss R, Garbi N, Sacher T, Arnold B, Hämmerling GJ. NK- and $CD8^+$ T Cell-Mediated Eradication of Established Tumors by Peritumoral Injection of CpG-Containing Oligodeoxynucleotides. J. Immunol., 167, 5247-5253 (2001).

[116] Garcia-Hernandez MD, Gray A, Hubby B, Klinger OJ, Kast WM. Prostate Stem Cell Antigen Vaccination Induces a Long-term Protective Immune Response against Prostate Cancer in the Absence of Autoimmunity. Cancer Res., 68, 861-869 (2008).

[117] Inoue J, Yotsumoto S, Sakamoto T, Tsuchiya S, Aramaki Y. Changes in immune responses to antigen applied to tape-stripped skin with CpG-oligodeoxynucleotide in mice. J. Control. Release., 108, 294-305 (2005).

[118] Nickoloff BJ, Turka LA, Mitra RS, Nestle FO. Direct and Indirect Control of T cell Activation by Keratinocytes. J. Invest. Dermatol., 105, 25-29 (1995).

[119] Cheng EM, Tsarovsky NW, Sonde PM, Rakhmilevich AL. Interleukin-12 as an in situ cancer vaccine component: a review. Cancer Immunol. Immunother., 1-9 (2022).

[120] Schmitz-Winnentha FH, Escobedo LVG, Beckhove P, Schirrmacher V, Bucur M, Ziouta Y, Volk C, Schmied B, Koch M, Antolovic D, Weitz J, Büchler MW, Z'Graggen K. Specific immune recognition of pancreatic carcinoma by patient-derived CD4 and CD8 T cells and its improvement by interferon-gamma. Int. J. Oncol., 28, 1419-1428 (2006).

[121] Zhang Y, Guan X, Jiang P. Cytokine and Chemokine Signals of T cell Exclusion in Tumors. Front. Immunol., 11, (2020) 1-20 (2020).

[122] Whitmire JK, Eam B, Whitton JL. Tentative T Cells: Memory Cells Are Quick to Respond, but Slow to Divide. PLoS Pathogens., 4, 1-11 (2008).

[123] Chaudhary N, Weissman D, Whitehead KA. mRNA vaccines for infectious diseases: principles, delivery and clinical translation. Nat. Rev. Drug Discov., 20, 817-838 (2021).

[124] He Q, Gao H, Tan D, Zhang H, Wang J. mRNA cancer vaccines: Advances, trends and challenges. Acta Pharm. Sin. B., 2969-2989 (2022).

[125] Lorentzen CL, Haanen JB, Met Ö, Svane IM. Clinical advances and ongoing trials on mRNA vaccines for cancer treatment. Lancet Oncol., 23, 450–58 (2022).

[126] Miao L, Zhang Y, Huang L. mRNA vaccine for cancer immunotherapy. Mol. Cancer., 20:41, 2-23 (2021).

[127] Kariko K, Whitehead K, Meel R. What does the success of mRNA vaccines tell us about the future of biological therapeutics?. Cell Syst., 757-758 (2021).

[128] Strategy to Achieve Global Covid-19 Vaccination by mid-2022. World Health Organization, Geneva., 2022.

[129] Pardi N, Hogan MJ, Porter FW, Weissman D. mRNA vaccines -a new era in vaccinology. Nat. Rev. Drug Discov., 17, 261-279 (2018).

[130]Wadhwa A, Aljabbari A, Lokras A, Foged C, Thakur A. Opportunities and Challenges in the Delivery of mRNA-based Vaccines. Pharmaceutics., 12, 1-28 (2020).

[131] Bidram M, Zhao Y, Shebardina NG, Baldin AV, Bazhin AV, Ganjalikhany MR, Zamyatnin AA, Ganjalikhani-hakemi J. mRNA-Based Cancer Vaccines: A Therapeutic Strategy for the Treatment of Melanoma Patients. Vaccines., 9, 1-33 (2021).

[132] Duan J, Wang Q, Zhang C, Yang D, Zhang X. Potentialities and challenges of mRNA Vaccine in Cancer Immunotherapy. Front. Immunol., 13, 1-7 (2022).

[133] Zhou WZ, Hoon DSP, Huang SKS, Fujii S, Hashimoto K, Morishita R, Kaneda Y. RNA Melanoma Vaccine: Induction of Antitumor Immunity by Human Glycoprotein 100 mRNA Immunization. Hum. Gene Ther., 10, 2719–2724 (1999).

[134] Miao L, Li1 L, Huang Y, Delcassian D, Chahal1 J, Han J, Shi1 Y, Sadtler K, Gao W, Lin J, Doloff JC, Langer R, Anderson DG. Delivery of mRNA vaccines with heterocyclic lipids increases anti-tumor efficacy by STING-mediated immune cell activation. Nat. Biotechnol., 37, 1174–1185 (2019).

[135] Huff AL, Jaffee EM, Zaidi N. Messenger RNA vaccines for cancer immunotherapy. J. Clin. Invest., 132, 2-12 (2022).

[136] Abe N, Imaeda A, Inagaki M, Li Z, Kawaguchi D, Onda K, Nakashima Y, Uchida S, Hashiya F, Kimura Y, Abe H. Complete Chemical Synthesis of Minimal Messenger RNA by Efficient Chemical Capping Reaction. ACS Chem. Biol., 17, 1308−1314 (2022).

[137] Hasan M, Hama S, Kogure K. Low electric treatment activates Rho GTPase *via* heat shock protein 90 and protein kinase C for intracellular delivery of siRNA. Sci. Rep., 9, 4114 (2019).

[138] Hasan M, Tarashima N, Fujikawa K, Ohgita T, Hama S, Tanaka T, Saito H, Minakawa N, Kogure K. The novel functional nucleic acid iRed effectively regulates target genes following cytoplasmic delivery by faint electric treatment.Sci. Technol. Adv. Mater., 17, 554-562 (2016).

[139] Hashimoto M, Takemoto T. Electroporation enables the efficient mRNA delivery into the mouse zygotes and facilitates CRISPR/Cas9-based genome editing. Sci. Rep., 5, 1-7 (2015).

[140] Wadhwa A, Aljabbari A, Lokras A , Foged C, Thakur A. Opportunities and Challenges in the Delivery of mRNA-Based Vaccines. Pharmaceutics., 12, 1-27 (2020).

[141] Clausen BE, Stoitzner P. Functional specialization of skin dendritic cell subsets in regulating T cell responses. Front. Immunol., 6, 1-19 (2015).

[142] Heine A, Juranek S, Brossart P. Clinical and immunological effects of mRNA vaccines in malignant diseases. Mol. Cancer., 20:52, 1-20 (2021).

[143] Bialkowski L, Weijnen A, Jeught K, Renmans D, Daszkiewicz L, Heirman C, Stangé G, Breckpot K, Aerts1 JL, Thielemans K. Intralymphatic mRNA vaccine induces CD8 T-cell responses that inhibit the growth of mucosally located tumours. Sci. Rep., 6:22509, 1-15 (2016).

[144] Chena J, Yea Z , Huanga C, Qiua M, Songa D, Lia Y, Xu Q. Lipid nanoparticle-mediated lymph node–targeting delivery of mRNA cancer vaccine elicits robust CD8+ T cell response. Proc. Natl. Acad. Sci. U.S.A., 119, 1-10 (2022).

[145] Haabeth OAW, Blake TR, McKinlay CJ, Waymouth RM, Wender PA, Levy R. mRNA vaccination with charge-altering releasable transporters elicits human T cell responses and cures established tumors in mice. Proc. Natl. Acad. Sci. U.S.A., 115, 9153–9161 (2018).

[146] Laczkó D, HoganMJ, Toulmin SA, et al. A Single Immunization with Nucleoside-Modified mRNA Vaccines Elicits Strong Cellular and Humoral Immune Responses against SARS-CoV-2 in Mice. Immunity., 53, 724–732 (2020).